NTNU

Norwegian University of
Science and Technology

Diagenesis and Reservoir Properties of Sandstones of the Battfjellet and Aspelintoppen formations from Nordenskiöldfjellet, Svalbard.

Hidaya Isaack Galiatano

Petroleum Geosciences
Submission date: July 2018
Supervisor: Mai Britt E. Mørk, IGP

Norwegian University of Science and Technology
Department of Geoscience and Petroleum

TPG4925 Petroleum Geoscience, Master's Thesis

Hidaya Isaack Galiatano

Master's thesis

Diagenesis and Reservoir Properties of Sandstones of the Battfjellet and Aspelintoppen formations from Nordenskiöldfjellet, Svalbard.

Trondheim, July 2018

NTNU

Norwegian University of Science and Technology

Faculty of Engineering

Department of Geoscience and Petroleum

NTNU

ABSTRACT

The Battfjellet and Aspelintoppen formations have been studied with the aim of finding textural and mineralogical properties of the sandstones and relate them to diagenesis processes and reservoir properties. The study was conducted with the aid of petrographic studies, where thin section samples from the Nordenskiöldfjellet area were analyzed by optical light microscopy and Scanning Electron Microscopy. The estimation of porosity was conducted with Imagej software.

Sandstones of the Battfjellet and Aspelintioppen Formation are chemically and textural immature composed with abundant quartz grains, mica and chert fragments together with minor amounts of feldspar, pyrite, epidote, rutile and zircon. The sandstones were observed with angular to sub angular grains and poor degree of sorting.

Mechanical compaction is the main diagenetic features that affected the sediments during the time of deposition and in their progress burial. Mechanical compaction was found to have much effect on the sediments as the sandstones were observed composed with ductile metamorphic fragment which were easily deformed during the compaction, hence porosity loss in these sandstones is mainly caused by the mechanical compaction.

The Battfjellet Sandstones show diagenetic alteration of clay minerals where kaolinite and chlorite have been observed as the most dominant clay minerals. They were found as pore filling and replacive minerals. Other diagenetic cement which are the result of chemical compaction have been found in very small trace amounts whereas calcite, siderite and quartz, illite cement were observed in the sandstone in both formations.

Porosity and permeability are the main features for a reservoir rock, and it is important to study these features to quantify the quality of the reservoir. Some of the Battfjellet Sandstones are characterized with coarse grains that show a moderate to good porosity with good pore connectivity. The fine-grained sandstones of the Aspelintoppen Formation do not serve as good reservoir as they have been found with very low porosity.

ACKNOWLEDGEMENT

First, I would like to acknowledge Professor Mai Britt Mørk of department of Geoscience and Petroleum for her guidance, advice and useful comments she put in this work. I recognize the help I received from her especially on proposing the outline of the repot, report writing skills and constructive ideas on diagenesis topic which have been covered in this report. The study would not have been possible without her significant inputs.

I would like also to express my gratitudes to Mr. Ernest Mulaya and Mr. Chone Rugangiza from University of Dar es salaam, Department of Geology for their contributions made in this thesis work, their important feedback and recommendation regarding report writting have been so useful and productive on this Master's thesis.

Lastly but not the least, I would like to recognise the support received form my family and friends. They have been of great help during the time of working on this thesis work. I am truly grateful for their patience and encouragement that they have shown me during the entire time of working on the thesis project.

TABLE OF CONTENTS

LIST OF FIGURES

LIST OF TABLES

ABBREVIATIONS

Alb	Albite
BEI	Backscattered Electron Image
Cal	Calcite
Cht	Chlorite
EDS	Electron Dispersive Spectrum
Ep	Epidote
Fds	Feldspar
Fm	Formation
Kaol	Kaolinite
Kfs	K-feldspar
Max	Maximum
MaxThr	Maximum Threshold
M-C	Medium to coarse grain
Min	Minimum
MinThr	Minimum Threshold
Msv	Muscovite
No	Number
NTNU	Norwegian University of Science and Technology
PPL	Plane polarized light
Pyt	Pyrite
Qtz	Quartz
R	Rutile
Sdr	Siderite

SEM	Scanning Electron Microscope
Sst	Sandstone
StdDev	Standard Deviation
Vf	Fluvial
XPL	Cross Polarised Light

1. INTRODUCTION

1.1 Location of the Study Area

Svalbard is an archipelago in the north western part of the Barents Sea, representing an uplifted and exposed part of the Barents Shelf (Figure 1). It has an area extension of only 63 000 km2 that is separated from Greenland and Franz Josef Land by a deep-water strait. Svalbard has been known as a gateway to the Arctic (Worsley, 2008; Kellogg, 1975; Kozak , et al., 2013). Svalbard has a complex geological evolution including Precambrian and Caledonian basement rocks as well as younger Palaeozoic, Mesozoic and Cenozoic sedimentary units. Various tectonic events have been documented affecting the geology of Svalbard, and the mentioned events are Late Precambrian, Caledonian and West Spitsbergen orogenies (Dallmann , 1999; Worsley, 2008).

The Central Tertiary Basin which is now onshore is found on south central part of Spitsbergen, it's development had involved the early phases of the opening of the Norwegian-Greenland Sea that occurred in Late Cretaceous to Eocene time (Talwani & Eldholm, 1997). The Spitsbergen is the largest island in the Svalbard archipelago. It has been argued that, the Central Tertiary Basin was a foreland basin based on its position found between the front of the west Spitsbergen fold belt and the adjacent craton (Helland-Hansen, 1990).

Several studies have found that the Central Tertiary Basin having an approximately 2 km thickness of Palaeocene-Eocene sedimentary succession that was deposited during the tectonic movement between the Greenland and Barents Sea blocks (Steel, et al., 1981) . A Facies study conducted by Helland-Hansen, (2010) have reported that, these Palaeocene-Eocene sediments were deposited mostly on coastal plains and wave or tide-dominated delta systems. Sediment infill in this basin is believed to originate from the up thrust of the west Spitsbergen flanks (Helland-Hansen, 1990; Steel, 1997). The sediments are characterised with both transgression and regression trends deposited in marine, deltaic and continental environment (Uroza & Steel, 2008). The Paleogene sediments show a progradation succession thinning towards East (Helland-Hansen, 1990).

Nordenskjöldfjellet is found onshore Spitsbergen and it has the sedimentation and facies style that are expected to be in the Barents Sea. The Nordenskjöldfjellet area is composed with the Battfjellet and Aspelintoppen Formations in the upper part of the Tertiary Central Basin, located on Spitsbergen not far from Longyearbyen (Figure 1). The thesis work will concentrate

mainly on the two formations (Battfjellet and Aspelintoppen) that are found in the Nordenskjöldfjellet Land. The findings that will be obtained in this study will give an opportunity of understanding the possible minerals (detrital & authigenic) and diagenetic reactions responsible for development of sandstones reservoir from these two mentioned formations.

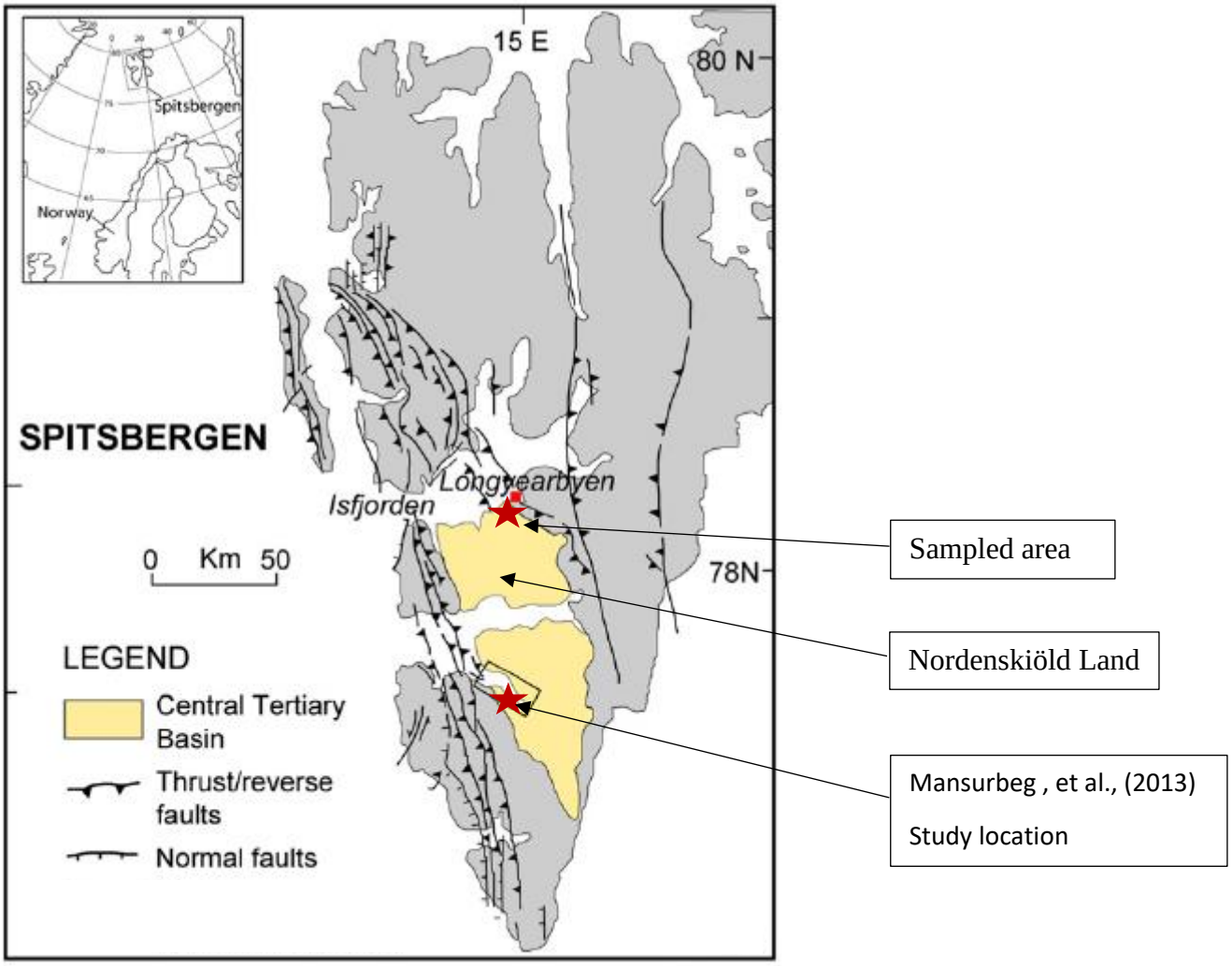

Figure 1: Location of Nordenskiöld-fjellet (sampled area) in Spitsbergen, Svalbard, a map from (Uroza & Steel, 2008).

1.2 Objectives of the study

The aim of this work is to study mineralogical composition and texture of the sandstones from the Battfjellet and Aspelintoppen formations, and the impacts of post-deposition processes. This will determine and highlight the detrital and diagenetic minerals found in these sandstones and deduce the responsible diagenetic processes that were involved in the development of the sandstones. The output from this study will be of great help on assessing the quality of these sandstones reservoir in relation to accumulation of hydrocarbons. Optical petrographic analysis and Scanning Electron Microscope (SEM) will be used as methods of obtaining the micro structural, mineralogical and textural information for the characterization of reservoir. These two methods have the ability of capturing microscopic features that can be used in understanding the detrital and diagenetic minerals together with the responsible compaction processes that have the effect on sandstone reservoir rocks.

1.3 Previous studies

Several scholars have previously studied the Battfjellet Formation (Mansurbeg, et al., 2013; Steel, 1977; Helland-Hansen, 2010; Uroza & Steel, 2008). Their findings have been of great help on understanding facies, sandstone mineralogical composition, detrital and diagenetic minerals and the occurred diagenetic processes and reactions. Here below is a summary of the findings that have been done by the mentioned authors.

Mansurbeg, et al., (2013) integrated diagenesis and sequence stratigraphy of the Eocene Central Basin, Spitsbergen Van Keulen Fjord area for understanding the distribution of diagenetic alteration and reservoir quality evolution in deep marine shelf sandstone. The observed controlling factors that were responsible for diagenetic alteration in the Eocene sandstones are detrital composition, burial depth and meteoric water flux. The article mentioned that, the Eocene Central Basin consists of falling stage and low stand system tracts, both systems have diagenetic alteration of kaolinite to illite, quartz overgrowth, carbonate cementation and kaolinization of detrital silicates. They also found that kaolinization of the detrital silicates is more dominate in the falling stage system tract, with the diagenetic alteration caused by percolating meteoric water in deep sea fan sandstone during relative fall of sea level. This explains the presence of kaolinite clay minerals in deep-water fan sandstone, interpreted as the effect of hydraulic head during relative fall of seal level. They also linked presence of kaolinite

with the regressive succession. Mechanical compaction played a big role in destroying primary porosity as the sandstone was composed with ductile grains which were easily deformed and that resulted in formation of pseudomatrix and loss of porosity. They also found that carbonate cementation (calcite and dolomite) was due to the presence of detrital carbonate grains which acted as source and nucleation site for the cementation. The carbonate grains were found below marine maximum flooding surfaces. Both eogenetic and mesogenetic alteration occurred in these sandstones as evidenced with kaolinization of mica and rock fragments developed in early diagenesis, and carbonate cementation observed developed in both early and burial diagenesis.

Steel (1977) did sedimentological studies on Battfjellet Formation on Nordenskjöldfjellet and found that, the formation was being composed of sandstone and siltstone deposited in a regressive mega sequence in marine environment. He described the Battfjellet Formation as a coarsening upward sequence. The coarser sandstones found in this formation were noticed with very low angle cross stratification originated in beach environment with the finer sandstone comprised with wave generated ripple lamination. He also found the formation being comprised with offshore transition zone sequences, barrier bar sequence, coastal lagoon tidal flat sequence, tidal channel complex and tidal flat sequence.

Helland-Hansen (2010) perfomed a study on facies and patterns of shelf deltas on the Eocene Battfjellet Formation located in Nordenskjöldfjellet Land. He did petrographic studies and X-ray diffrraction analysis to identify and quantify minerological composition of the Battfjellet Sandstones. The petrographic analysis found that the sandstone are of poor to very poor sorting, and with angular to sub-angular grains, and were composed with grains of quartz, chert, feldspar, organic detritus, carbanaceous detritus, rock fragments, shale and some authigenic clay. He discovered several facies that were representing a wave dominated shelf delta in which the sediments were deposited in a regression succession. He also combinned the sedimentary facies, sediment composition and parasequence stacking pattern and suggested the Battfjellet Formation is of a fluvial-wave intercalation delta origin.

The Battfjellet Formation has also been interpreted as part of a prograding delta that include 20 sand-prone, eastwards prograding, shelf-margin clinoforms (Steel & Olsen, 2002; Uroza & Steel 2008). Uroza and Steel (2008) focused their study on clinoform 17 which is representing a sand rich delta with a progradation succession of both falling and rising of relative sea level (Figure 4). They did a fieldwork by measuring 18 verticle sedimentary profiles, outcrop photographing and studied gamma-ray profiles. They were able to map the sandbody

geomentry and succeded on characterizing the delta profile and its associated facies. The associated facies were then compared with the gamma-ray responce. They concluded the Clinoform 17 of the Eocene Battfjellet Formation was developed during the highstand condition as it was evendenced with thick aggradation and parasequence-prone sequence. They also suggested the Clinoform 17 was deposited in a wave dominated environment that were deposited on the coastal plain and shelf margin.

1.4 An overview on diagenesis

Diagenesis encompasses the physical, chemical and biological processes that react with the sediments and their interstitial water in a sedimentary basin to attain textural and mineralogical equilibrium in response to change in environment from deposition to metamorphism. Or in another way, diagenesis can be referred to all the processes that are responsible for the development of sediments into rocks, and these processes include mechanical compaction, grain dissolution and precipitation of authigenic minerals. There are several parameters that are necessary for these processes to happen and affect the sediments during their deposition and burial phases, such parameters are temperature, pressure, composition of pore fluid and type of detrital grains deposited. The increase of temperature and pressure tends to facilitate formation of diagenetic minerals due to most of minerals become unstable on rising of temperature (Worden & Burley, 2003).

Diagenesis have been categorised into three regimes known as eogenesis, mesogenesis and telogenesis. These three categories are differentiated in terms of physical and chemical reactions involved and the burial depth of the sediments (Worden & Burley, 2003; Bjørlykke & Jahren, 2010).

Eogenesis which is also known as early diagenesis occurs at shallow depth of l to 2 km with the temperature ranging from surface temperature to 70 °C depending on depth and the geothermal gradient of the sedimentary basin. Sediments react with air and water that lead to the change of primary textural and mineralogical composition, the process known as near surface diagenesis. The chemistry of interstitial water is responsible for these changes in sediments which is controlled with the deposition environment which depends on climate. This regime encompasses weathering and soil development in continental environment and biogenic redox reaction in marine environments (Worden & Burley, 2003; Bjørlykke & Jahren, 2010).

Mesogenesis (Burial diagenesis) occurs at depths of greater that 1 to 2 km and with maximum temperatures ranging between 200 to 250 °C. It involves physical and chemical processes occurring in sediments during burial that are responsible for several modifications found in the sedimentary rock. The major controlling factors on the chemical reactions that are occurring in this regime are the increase of temperature, pressure and changes in pore water chemistry as most of minerals become unstable due to the increase solubility. Pressure dissolution tend to occur in these conditions whereby detrital silicate minerals such as quartz dissolve on contacting with clay minerals. The dissolved silica will tend to precipitate as overgrowth on detrital quartz grains and reduces porosity in reservoir sandstone. The other diagenetic reactions that occur during burial are replacement of smectite to illite, formation of illite from the reaction between K-feldspar and kaolinite, dissolution of K-feldspar and precipitation of and carbonate cements. Kaolinite may change to dickite and chlorite on increase of temperature given there is scarcity availability of potassium (Bjørlykke & Jahren, 2010; Worden & Burley, 2003).

The chemical compaction will continue even during uplift if the temperature remains greater than 70◦C (Figure 2).

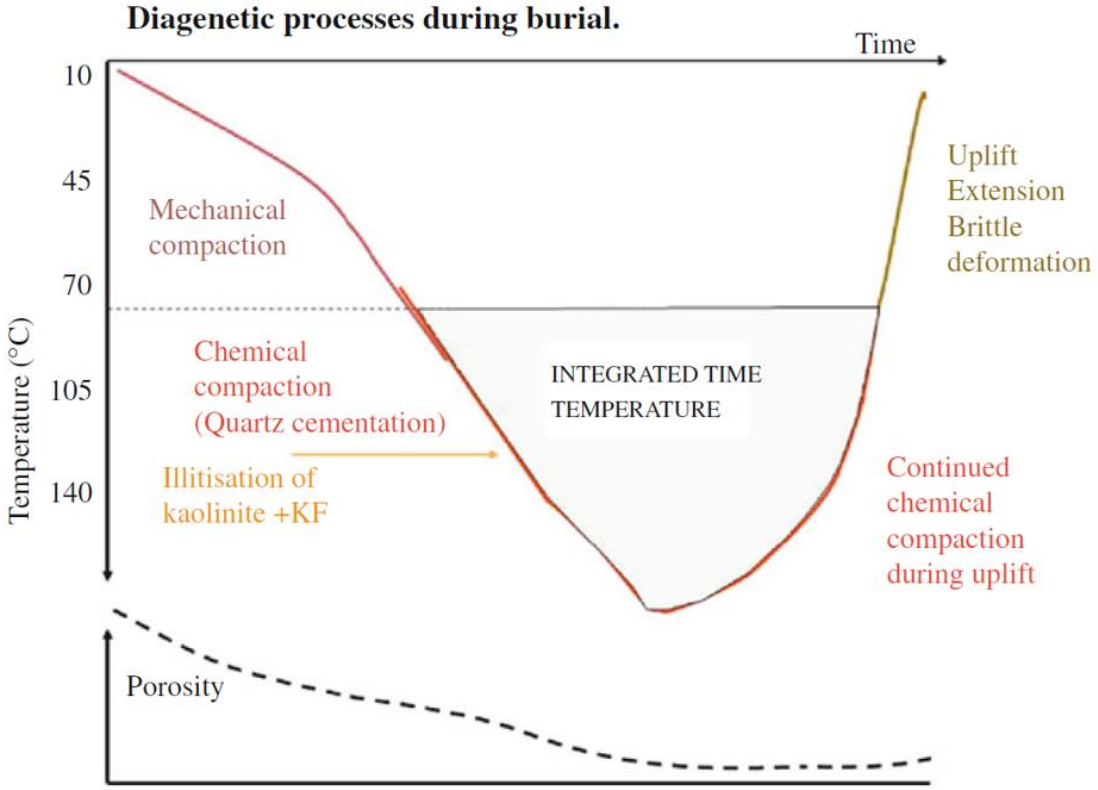

Figure 2: A sketch of diagenetic processes that are occurring during development of sedimentary rocks (Worden & Burley, 2003).

Telogenesis occurs in uplifted rocks (Figure 3) which have been exposed to meteoric water, normally carbonate rock and cement are dissolved and reprecipitate in other part of sedimentary rocks in a basin. If feldspar is present, it can react with meteoric water to generate kaolinite. These geochemical reactions occur when meteoric water percolating in uplifted sedimentary rocks. The chemistry of meteoric water is what facilitates telogenic processes as the meteoric water is always composed with CO2 which makes it to have low acidity and low salinity (Worden & Burley, 2003). Most of telogenic reactions occur within the first 10 meters below sediments surface.

Figure 3 summarises the regimes of diagenesis and shows important parameters that are necessary for occurrence of these diagenetic regimes in a sedimentary basin.

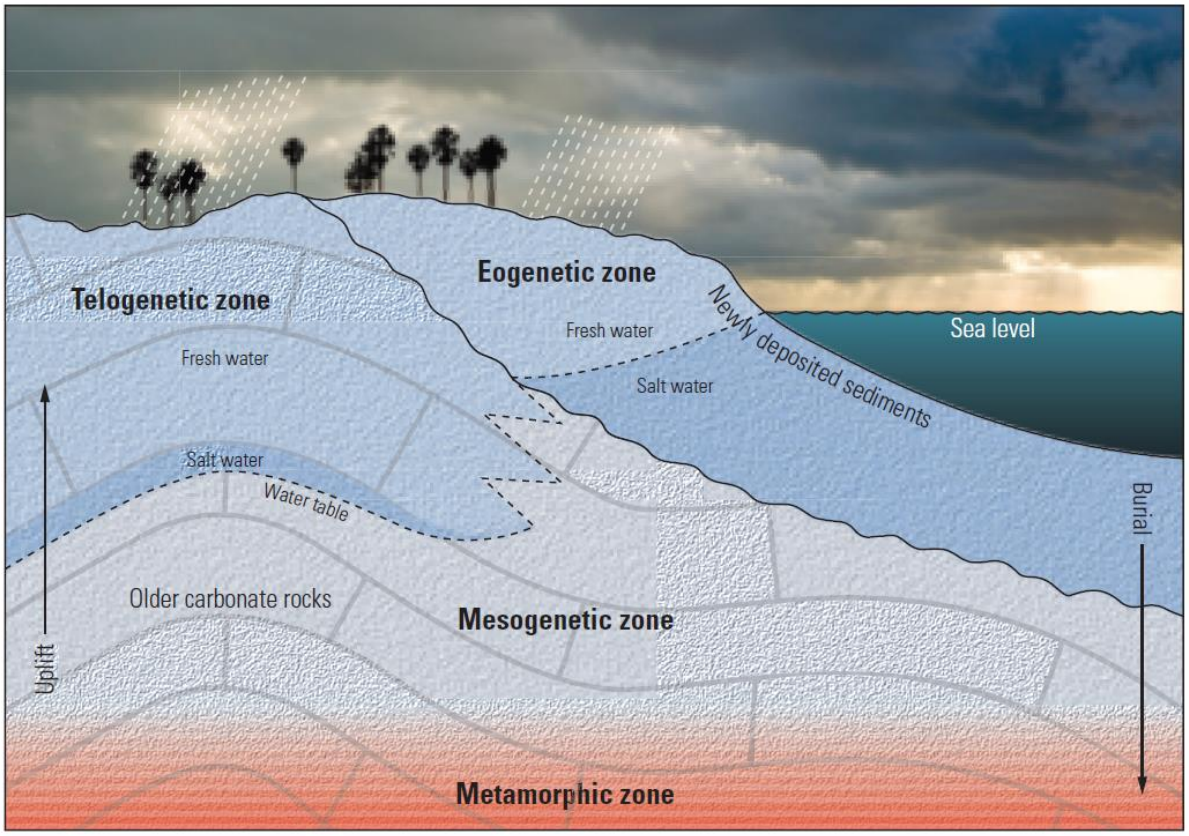

Figure 3:A schematic diagram with different regimes of diagenesis which have a close relation with deposition, burial of sediments and rock uplifting (Ali, et al., 2010).

1.5 Reservoir quality

The most important properties for any reservoir are porosity and permeability that determine the accumulated hydrocarbons in place. Porosity has been defined as total volume of voids in a rock and is expressed in fraction or percentage of total volume of rock. It has been categorised into primary and secondary type depending on mechanism that were responsible for their occurrence.

Primary porosity which is also known as deposition porosity is the intergranular volume originated during deposition of sediments. Primary porosity is determined by important parameters such as packing of grains, sorting of grains and the grain shape. Well sorted sandstones have higher porosity than correspondingly sized of poorly sorted sandstones as poor sorted sandstones are always composed with very fine-grained particles that fill the intergranular spaces and reduce porosity.

Normally a clean well sorted sand is deposited with porosity around 40%, and after undergoing compaction which include physical and chemical compaction it can be found with porosity of up to 30-25%. Sandstone composed with ductile minerals such as clay minerals, metamorphic grains, volcanic grains and mud intraclasts loose porosity relatively easy during compaction as they deformed more easily than rocks composed of rigid rock fragments (Worden & Burley, 2003).

Secondary porosity also known as post depositional porosity is the one which occur as the results of dissolution and leaching of primary detrital grains, matrix and already crystallized cement (Worden & Burley, 2003). It can also be developed by tectonic activities which result in fracturing and faulting in associated rock. It has been documented to occur in all regimes of diagenesis such as eogenesis, mesogenesis and telogenesis whereby chemical, physical, biophysical process are playing important role on developing these secondary pores (Volkmar & David, 1979)

Most of secondary porosity is forming during burial, their development is associated with diagenetic processes that are responsible for dissolution of K-feldspar and leaching of carbonate grains and cements (Worden & Burley, 2003). Decarbonization occurred in mesogenesis is due to availability of CO_2 from decarboxylation reaction that is responsible for formation of carbonic acid (Volkmar & David, 1979). Feldspar leaching and formation of secondary porosity in sandstones also take place at shallow burial depths by flushing with meteoric waters (Bjørlykke, et al., 1992).

Secondary sandstone porosity has been reported to have a great potential on the accumulation of hydrocarbons as its volume is found to exceed most of the primary sandstone porosity at great burial depth. As what have been observed in Prudhoe bay field and the Jurassic field reservoir in the North Sea, the giant accumulation of hydrocarbons has been reported in this deep sandstone reservoir (Volkmar & David, 1979).

To predict quality of the reservoir there is a need of understanding diagenesis processes and sequence stratigraphy of the interesting formation (Mansurbeg, et al., 2013). This will help on predicting porosity at a given depth. Normally, porosity relate to primary depositional porosity, textural and minerology composition of sediments, burial depth, growth of authigenic minerals and responsible compaction processes (Bjørlykke & Jahren, 2010; Worden & Burley, 2003).

2. CENOZOIC GEOLOGY OF SVALBARD

The Tertiary tectonic history of Svalbard is well known as several studies have been conducted before with the aim of understand the geology of the area (Kellogg, 1975; Muller & Spielhagen, 1990; Steel, et al., 1985). The major tectonic events which were responsible for this development are, (1) North-North Western movement of Greenland from the Eurasia plate and (2) West-Northwestern movement which was caused by the change of pole rotation (Steel, et al., 1985) occurred in the geological time that resulted in strike-slip movement and uplifting.

The Central Tertiary Basin of Spitsbergen was formed along the strike-slip boundary between Greenland and the Eurasian plates in late Cretaceous to Paleogene. Dextral shearing forces were responsible for the development of the Tertiary Central Basin. The evolution of the Svalbard Geology and the Central Tertiary Basin occurred in four phases with different processes as what have been proposed by Muller & Spielhagen, (1990).

The phase one was associated with strike-slip movement, with Trolle Land fault system assumed being the plate boundary between Greenland and Svalbard in the late Cretaceous. The plate boundary was override Hornsund Fault zone in eastward direction in early Palaeocene. A short sinistral strike-slip phase was responsible for the movement between Greenland and Svalbard in early Palaeocene that resulted in doming, uplift and slight tilting of the Barents Shelf. The tectonic events are evidenced by the absence of Cretaceous sediments as they were eroded during the uplift (Muller & Spielhagen, 1990).

Phase two was dominated by compression forces between Svalbard and Greenland in late Palaeocene to early Eocene which resulted in sea floor spreading along the western margin of Spitsbergen. The west Spitsbergen Fold Belt was the result of this compression event. The fold is characterised with high angle reverse faults, thrust fault and asymmetrical thrust ramps structures (Muller & Spielhagen, 1990).

Most of the crustal shortening was due to transpression process caused by compression between the two plates, the mechanism observed occuring in phase three of the development of Svalbard and Central Tertiary Basin. Dextral movement was the result of the transpression event occurred between Svalbard and Greenland occurred in 56 Ma to 49Ma (Muller & Spielhagen, 1990).

Strike slip motion occurred in lower middle Eocene where by Greenland and Svalbard experienced this movement followed by rifting which resulted in sea floor spreading and the development of Svalbard. This event mark phase four of tectonic development in this area. It is believed that the tectonic and sediments developments in the Central Tertiary Basin have been resulted from rifting and seafloor spreading between Greenland and Eurasia (Muller & Spielhagen, 1990). And the western Spitsbergen orogeny evolved due to a large scale transcurrent motion between Greenland and Eurasia plates that led in opening of the Norwegian sea (Steel, et al., 1985). According to Helland-Hansen (1990) the major fault activities observed in the area were the ones responsible for strike-slip event between Greenland and Svalbard in late Palaeocene.

3. SEDIMENTOLOGICAL DESCRIPTIONS

3.1 Stratigraphy and Basin Infill

The Van Mijenfjorden Group (Figure 5) has succession of sediments of Paleogene time deposited in the Central Tertiary Basin in two episodes. The lower succession part which consists of the Firkanten and Basilika formations was the first being deposited in the deposition history in the Central Tertiary Basin. The sediments were originating from east, west and north and showing a generally transgression trend (Helland-Hansen, 1990). Marine clastic sediments and coal were also deposited (Kellogg, 1975). Later, the period of regression was the one responsible for deposition of the upper part of the Basilika Formation and the Grumantbyen Formation where in this case the sediments source was from north and north-east (Helland-Hansen, 1990). Fine-grained sediments of the Gilisonryggen Formation were then deposited during the rise of sea level in a transgressive sequence. Deposition of these sediments were associated with uplift of the west margin of the basin (Kellogg, 1975).

The sedimentation of the Van Mijenfjorden Group was terminated by a regression pattern that was responsible for deposition of the Gilsonryggen, Battfjelet and Aspelintopen Formation (Helland-Hansen, 1990).

3.2 Van Mijenfjorden Group

The Van Mijenfjorden Group consists of seven formations that are the Firkanten, Basilika, Grumantbyen, Frysjaodden, Hollendardalen, Battfjellet, and Aspelintoppen deposited in Palaeocene and Eocene time (Figure 5). The sediment infill in the Tertiary Central Basin which form the Van Mijenfjorden Group has the thickness of around 2.3km (Steel, et al., 1985). This Paleogene succession consisting of clastic sediments thinning towards east (Helland-Hansen, 1990).

The Van Mijenfjorden Group is characterised with a lower succession that consists of the Firkanten, Basilika and Grumantbyen formations deposited in early to mid-Palaeocene. And the upper succession is composed of the Hollendardalen, Battfjellet and Aspelintoppen formations that are forming a regressive mega sequence with a thickness of 1.5km (Steel, et al., 1985).

The Battfjellet and Aspelintoppen formations will be discussed into the details as this study involves petrographic analysis of the polished thin section samples from these two formations.

3.2.1 Battfjellet Formation

The Battfjellet Formation is composed of shoreline sediments with a coarsening upward sequence varying in thickness from less than 60 m in the northeast to about 300 m south of Van Mijenfjorden. The formation was deposited in a regression sequence comprising shallow marine and estuary sediments. It is underlain with shale of the Frysjaodden and overlain by the Aspelintoppen Formation (Figure 5) (Steel, 1977). Wave generated sedimentary structures are found in the lower part of the upper sandstone documented marginal part of the formation as evidenced by hummocky cross stratification, and horizontal and wave ripple laminations. Furthermore, well developed stratification structures with lateral variation and diachronous in nature were identified characterise the formation (Helland-Hansen, 201; Steel, 1977).

Siltstones and sandstones beds of marine origin have been observed in this formation. The sandstone is of light grey colour with poorly sorted grains and some metamorphic fragments, weathered feldspar and carbonaceous grains originated from Spitsbergen thrust fold (Kellogg, 1975). Grain size varies from fine to medium in the lower part of the formation to medium to coarse in the upper part of the formation. Some of the sandstone beds and group have been observed thinning out laterally toward east (Steel, 1977).

The Battfjellet Formation represents an Eocene delta protruded into the shelf margin of the Eocene Central Basin. The delta was developed during relative rise and fall of the sea level and is characterised with shelf margin 4^{th} order clinoforms protruding into marine environment (Figure 4). Clinoform 13 and 14 show a flat trajectory which indicate a very stable falling of the sea level whereas the trajectory of clinoform 16 and 17 have high slope implying relative rising of the sea level (Figure 4); (Uroza & Steel, 2008).

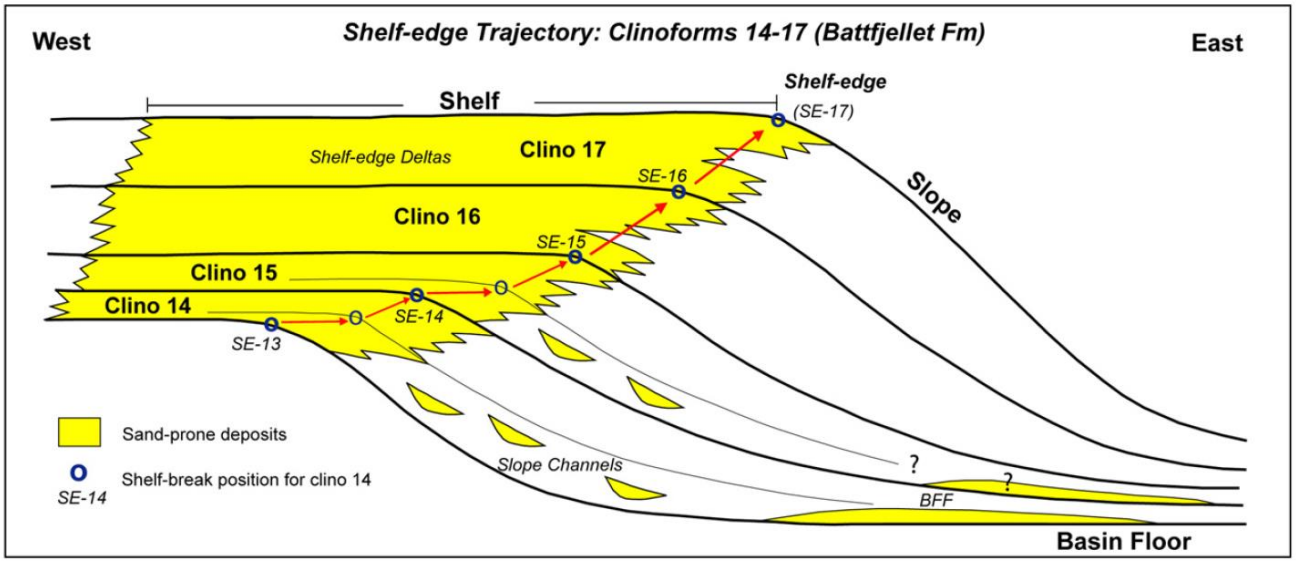

Figure 4: A sketch of the Eocene delta trajectory of Battfjellet Formation showing clinoform 14 to 17(Uroza & Steel, 2008).

Several lithological facies have been observed suggesting different processes and mechanisms of deposition of sediments. The observed facies are offshore, offshore transitional, lower shoreface, middle shoreface and upper shoreface. The following is the summary of the facies found in the Battfjellet Formation.

The Offshore facies identified in the Battfjellet Formation, it is composed of massive bodies of shale, mudstone and siltstone with the fine sandstone on top of the facies. It is interpreted as deep shelf facies contains fine sediments deposited in marine environment. Coarsening upward sequence has been identified as one of characteristics of this facies (Helland-Hansen, 2010).

The Offshore transitional facies is comprised with alternation of fine sandstone and mudstone layers. A fine sandstone unit is found on top of the facies shown with hummocky cross stratification, wave ripple marks and bioturbation. The facies was deposited in the offshore transitional zone dominated by moderate wave and storm wave activity (Helland-Hansen, 2010).

The Lower shoreface facies is composed of alternating wave ripple lamination and horizontal lamination of very fine to fine sandstone layers. The facies has been deposited in a moderate energy environment (Helland-Hansen, 2010).

The Middle shoreface sands facies is another facies found in the Battfjellet Formation, it is composed of fine sandstone deposited in wave dominated environments (Helland-Hansen, 2010).

The Upper shoreface sands also found in the Battfjellet Formation consists of interbedded sandstone sets with horizontal or low angle lamination and tabular cross stratification deposited in an environment of unidirectional and shifting currents (Helland-Hansen, 2010).

3.2.2 Aspelintoppen Formation

Aspelintoppen Formation is comprised with non-marine continental sediments deposited in a deltaic plain system. It is the uppermost and youngest formation in the Van Mijenfjorden Group with approximately thickness of about 1000 m. This sedimentary succession was deposited in a regression sequence (Kellogg, 1975).

The formation consists of very fine and poorly sorted sandstone, calcareous shale, claystone plant remains and coal giving evidence of terrestrial sediments. The plant remains are plants debris, coal, petrified tree limbs and trunks (Kellogg, 1975; Steel, et al., 1981). The sediments have been deposited in low-sinuosity streams at a very low angle (Helland-Hansen, 1990). Both coarsening and finning upward sequences have been observed characterising this formation. The formation has soft deformation structures that are forming very fine lamination and fold structures with the amplitudes up to 2m. These structures were the results of frequent occurrence of earthquakes and high sedimentation rate during tectonic activities (Steel, et al., 1981).

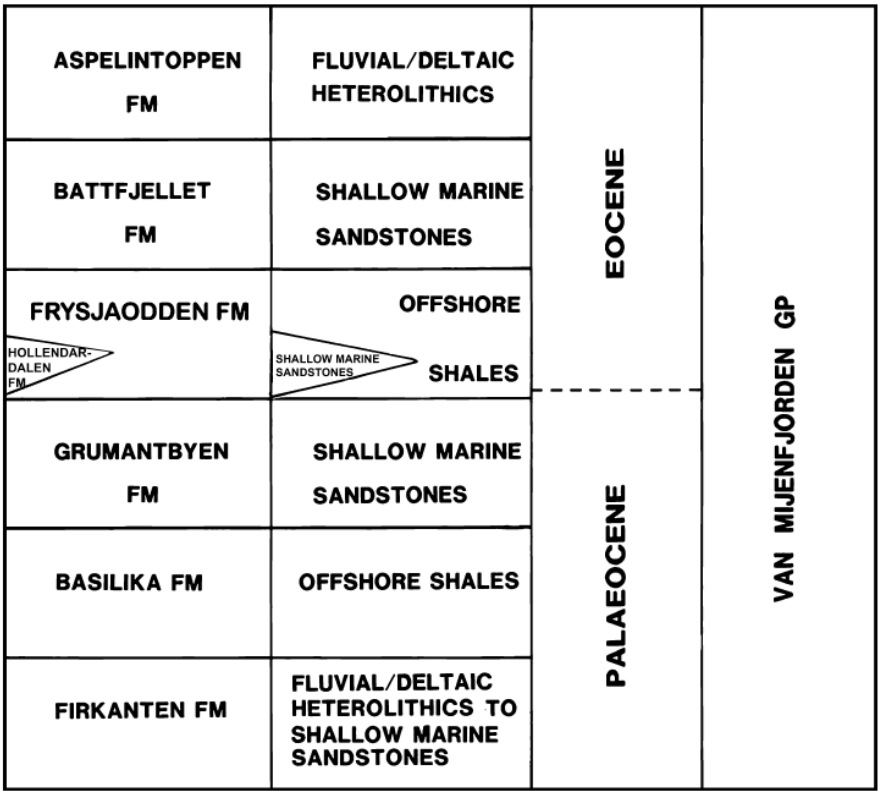

Figure 5: The Van Mijenfjorden Group of Tertiary Central Basin with Paleogene Succession with the deposition style of the sediments (Helland-Hansen 2010).

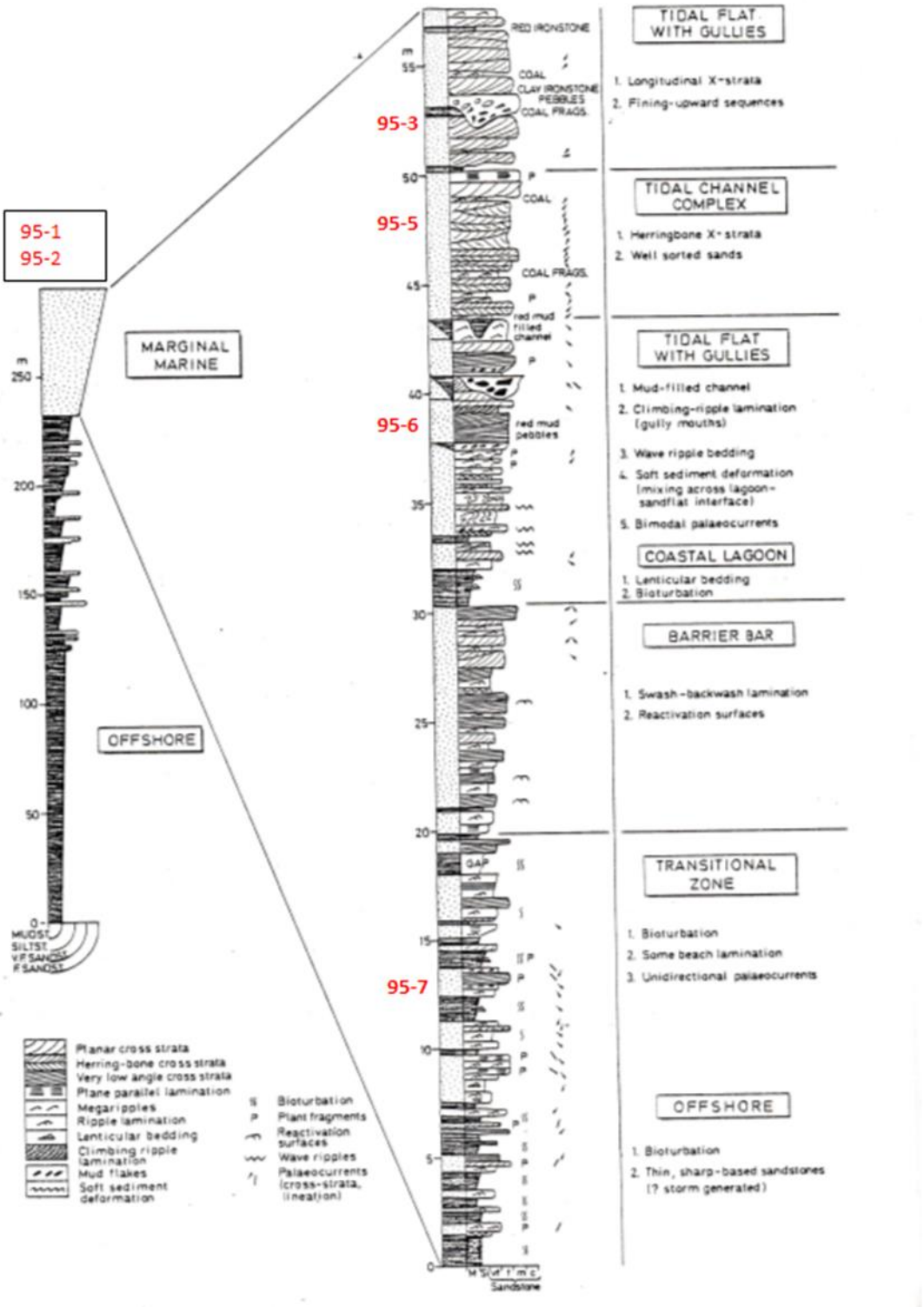

Figure 6: Sedimentological log of the Battfjellet Formation at Nordenskjöldfjellet from Steel (1977). Sample numbers for this study are shown in (95-) series.

4. METHODOLOGY

This chapter covers the methods that were used to study petrography and mineralogical composition of the sandstones of the Battfjellet and Aspelintoppen formation. Porosity estimation conducted on polished thin sections is also described in this chapter. The chapter will also mention how the samples were collected and prepared for petrographic study.

4.1 Sampling

Seven polished thin sections samples of sandstone from Nordenskiöldfjellet, Svalbard were sampled by Mai Britt E. Mørk in 1995 (Table 1) by referring to the sedimentology log that was prepared by Steel, (1977). Samples were collected at the same stratigraphic heights in the log as what is shown in Figure 6. Then polished thin sections were prepared for the petrography study and blue coloured epoxy was used to show porosity. The sedimentological descriptions that is found in (Table 1) has been used as the guide while interpretang minerals that were observed in polished thin section samples during petrographic observeation.

Table 1: Sample collected from Nordenskiöldfjellet land.

Sample no	Sample reference*	Lithology	Formation
95-1	Above log	Sst with plant fragments	Aspelintoppen Fm.
95-2	c. 5m above fm. basis	Sst, fine-grained	Aspelintoppen Fm.
95-3	c. 56 m	Sst, M-C-grained, above channel	Batfjellet Fm.
95-4	c. 55 m	Sst, with coal fragments, channel fill	Batfjellet Fm.
95-5	47 m in log	Sst with crossbeds	Batfjellet Fm.
95-6	38 m in log	Sst, low angle crossbeds	Batfjellet Fm.
95-7	13 m in log	Sst, Vf, thin laminated	Batfjellet Fm.

The following are the summary of the lithofacies of the samples collected at Nordenskiöldfjellet area. The description of facies was conducted by Steel (1977).

The Offshore-transitional zone sequences found at height 0-245 m (Figure 6) is represented by sample number 95-7. The sandstones of this facies was observed with monotonous sequence of dark, silty marine shales composed of chert fragments. Fine-grained sandstones were identified in this zone with some showing ripple lamination, massive, soft deformation and some bioturbation. Plant fragments, thin layer of conglomerate and asymmetric wave-ripples is also found on the upper part of this lithofacies. The evidence such as fine nature of sediments observed, and the presence of burrowing organism show this zone was deposited in offshore environment.

The barrier bar sequence which is found at height of 245-256 m (Figure 6) and is represented by sample number 95-6. The facies is characterised with a well sorted sandstone with a coarsening upwards sequence, some mudstone and siltstone are also found in this zone. The structures observed in here are plane parallel lamination/ very low angle cross-stratified sets. This zone was suggested to have deposited in high energy regime possibly in a beach environment. The succession has been divided into four categories known as foreshore deposits, upper shoreface deposits, lower shoreface deposits and farther offshore.

Sample number 95-5 collected from facies of the coastal lagoon-tidal flat sequence found at height of 256-269 m (Figure 6) has been marked being dominated with poor sorted sandstones. There is an alternating layer of well and poor sorted sandstone in this succession which suggests tidal and beach deposits. The interchanging of sediments/sandstones has been marked with white and yellow colour with the white colour representing a well sorted sandstone. Another reason this succession has been proposed being deposited in tidally and beaches setting is its stratigraphy position found in between a barrier bar sequence and a tidal channel complex. The poor sorted sandstone was resulted from the mixing of lagoonal muds with well sorted sand.

Sample number 95-4 shown in Table 1 was collected in the tidal channel complex facies which is found at height of 269-276 m (Figure 6). The facies is composed with a well sorted, medium grained sandstones characterised with cross stratification structures found with coal fragments. Some plant remains have been observed in the coarse-grained sandstone located at the top of this succession.

Sample number 95-3 of the tidal flat sequence that is found at the top of the Battfjellet Formation at Nordenskjöldfjellet (height 276-284 m) as shown in Figure 6 has herringbone

cross-strata, coal fragments and mud deposits. The findings have suggested these sandstones to have been deposited by the influence of tidal currents.

The coastal plain deposits facies of the Aspelintoppen Formation consist of fine sandstone and shale with low sand-shale ratio. Sample number 95-2 represent the mentioned facies whereby sandstones found are characterised by soft sedimentary deformation structures and accumulation of organic matter in the sediments. Carbonaceous mudstone and coal are also present in this facies. A coarsening upward sequence characterise the facies where by up to 4m of fine to medium coarse-grained sandstone have been identified. The sediments were deposited in a bay as the result of over-flow of the river banks. The source of sediments was of distributary channel (Helland-Hansen, 2010).

And lastly, sample with number 95-1 represent the tidally influenced facies that is found in the Aspelintoppen Formation. The facies consists of fluvial and tide dominated estuary deposits (Helland-Hansen, 2010). The analysed sandstones were identified comprising plants fragments Table 1.

4.2 Optical light microscopy (Petrography)

The study involved petrographic descriptions of seven polished thin section samples by using transmitted light microscope under both plane and cross polarized light. Petrographic study was done in three weeks during Summer in 2017 as part of my specialization project (Galiatano, 2017) at the Norwegian University of Science and Technology, in the Geology building. Mineral grains, rock fragments and sandstone texture were identified, and the results are documented in (Table 3). Optical micrographs provide important information of mineralogical composition, texture and sedimentological features that are very important on identifying and understanding the diagenetic processes and alterations that have a huge effect in the quality of the reservoir sandstone.

4.3 Scanning Electron Microscopy (Petrography)

Scanning Electron Microscopy was conducted in spring on sample numbers LY95-3, LY95-5 and LY95-6L by K. Erikson and MBE Mørk at department of Geoscience and Petroleum, NTNU and all data were interpreted by myself at the University of Dar es salaam. The SEM analysis was conducted to identify the minerology composition that are found in the sandstone samples of the Battfjellet Formation. The method was conducted as a supplementary method to optical petrography with the purpose of correctly identifying the mineralogy composition. The advantage of this method is that can enable the interpreter to identify the fine-grained clay minerals as sometimes can be trick identified in optical microscope.

The SEM BEI analysis have verified texture and composition of detrital, diagenetic minerals and some diagenetic features that are very important in assessing reservoir quality.

The identification of minerals in the polished thin section samples was conducted by studying the elemental composition using Energy Dispersive Spectral (EDS) analysis.

Backscattered Electron Image (BEI) was used to differentiate the minerals that are found in thin section samples based on atomic weight / density contrast. BEI image analysis is very good at identifying textural relation and mineral zoning in a polished thin section. The minerals in BEI images are shown with different grey colour due to the response of atomic weight or density. The minerals with high to medium density are shown with light colours, while minerals with low density are displayed with a dark colour. For example, a heavy mineral such as zircon was found with a light colour (Figure 20) while the low-density minerals such as quartz were found in a dark colour (Figure 17).

4.4 Imagej Porosity Estimation

The porosity estimation was conducted with help of Imagej software on sample number LY95-3 and LY95-5 that are representing the sandstones of the Battfjellet Formation. The software involved on calculating area fraction of open spaces in this section sample which in this case is known as porosity. The porosity is shown with grey colour in the white and black images that are found in Appendix (Figure 49; Figure 50; Figure 51 ; Figure *52*), the images have been displayed with the similar original optical petrography images to show the porosity available in thin section samples. The white and black images were converted from the optical

micrography (plane polarized) to be used on imagej software as the software works better with black and white jpeg images.

Similarly, the calculation of porosity was conducted on Backscattered Electron Images (BEI) with porosity shown in black colour (Appendix in Figure 53& Figure 54). All the images used for the calculation of porosity were of Battfjellet Formation. The porosity is identified with black colour because of no any density available in the area as porosity is presented with volume of voids.

Note lower porosity values in analyses LY95-3_1 to LY95-5_2 using SEM BEI (Table 2) comparing to the analysis performed on optical micrography images (LY95-3 and LY95-5).

Table 2: Results of porosity calculated using Imagej software.

Sample No	Area	Mean	StdDev	Mode	Min	Max	Median	**%Area**	MinThr	MaxThr
LY95-3	235934	136.18	12.76	150	112	156	138	**12.29**	112	156
LY95-3	248718	135.89	12.42	148	112	156	137	**12.95**	112	156
LY95-3	201043	135.21	12.44	139	112	156	136	**10.47**	112	156
LY95-5	260606	137.67	13.07	152	112	156	139	**13.57**	112	156
LY95-3_1	1.56	14.63	24.9	0	0	63	0	**8.31**	0	63
LY95-3_2	2.05	24.39	27.83	0	0	63	0	**10.93**	0	63
LY95-5_1	1.64	18.24	28.39	0	0	67	0	**8.72**	0	67
LY95-5_2	2.08	25.49	28.57	0	0	63	0	**11.09**	0	63

5. RESULTS

This section presents the results obtained from petrographic studies that were carried out on the polished thin section samples of the Battfjellet and Aspelintoppen Formation. The interpreted results are summarized in the following table 3 and 4 found below.

Table 3: This table summarizes the results obtained from optical petrography

Sample No	**Detrital Minerals**	**Diagenetic Minerals**	**Grain Size**	**Sorting**	**Shape**	**Maturity**	**Formation**
LY95-1	Quartz, mica, chert.	Calcte, siderite.	0.05mm-0.125mm Fine grained	Well sorted	Subrounded	Fine grained immature sandstone	Aspelintoppen
LY95-2	Quartz, chert, mica, plagoclase.	calcite	0.05mm-0.165mm Fine grained	Well sorted	Very angular to angular	Fine grained immature sandstone	Aspelintoppen
LY95-3	Quartz, mica, plagioclase, chert, glauconite, and other rock fragment.	Pyrite, quartz and calcite.	0.2mm-0.55mm medium to coarse grained	Moderate to poor sorted	Subrounded with low spericity	Immature Sandstone	Battfjellet
LY95-5	Quartz, feldspar, chert, mica, chalcedony.		0.17mm-0.35mm medium to coarse grained	Modreate to well sorted	Subangular	Immature Sandstone	Battfjellet
LY95-6-L	Quartz, plagioclase, chert, mica,	Siderite	0.125mm-0.25mm Fine grain	Moderate sorted	Angular to subangular	Fine grained	Battfjellet

	tourmaline, heavy mineral, chlorite fragment.					Immature Sandastone	
LY95-6-T	Mica, chlorite, plagioclase, chert, some heavy mineral.	Calcite	0.1mm-0.25mm Fine grain	Poorly-sorted	Angular to subangular	Fine grained immature Sandstone	Battfjellet
LY95-7	Quartz, feldspar, rutile, mica, mica schist aggregates and pyrite.	siderite and pyrite	0.06mm-0.09mm Fine grain	Moderate sorted	Subangular	Fine immature Sandstone	Battfjellet

5.1 Samples Description

Sample LY95-7 was observed dominated with fine-grained sandstone as what have been illustrated by Steel (1977). The sandstone sample was collected from the Transitional zone Figure 6. The sandstone analyzed on polished thin section was identified with a moderate sorting with most of its grains possessing subangular shape.

Sample LY95-6-T of the analyzed sandstone was observed with angular to sub angular shape corresponding to the coastal lagoon- tidal flat sequence by Steel (1977). He described the sandstones of this facies as different from the underlying beach environments (Figure 6).

Sample LY95-6-L was identified with moderate sorting with angular to sub-angular grains. These facies is described by Steel (1977) (Figure 6) as the result of the mixing of lagoonal muds with well sorted sands. The sandstone sample was collected from Tidal flat facies which is characterized by mud filled channel deposits with some ripple laminations.

Sample LY95-5 observed with medium to coarse-grained size dominated with sub angular grains. The sample was collected from Tidal channel complex facies (Figure 6). The degree of sorting was recognized being of moderate to well. All the identified feature in this sandstone facies agree with the ones described by Steel (1977).

Sample LY95-3 collected from Tidal flat facies was identified with sub-rounded mineral grains, the degree of sorting was observed being poor to moderate as mixing of different sizes of grains were noted. The sandstone was also observed containing medium to coarse grain-size. Steel (1977) described the facies to contain finning upward sequence composed of longitudinal x-strata.

Sample LY95-2 and LY95-1 are from the Aspelintoppen Formation and they were analyzed composed with quartz, mica, chert and feldspar. The sandstones analyzed are from coastal plain and tidally influenced deposits. These samples were collected above of the Battfjellet Formation in the same vertical section on the Nordenskiöldfjellet mountain as what is shown in (Figure 6).

5.2 Optical petrographic result on Battfjellet Formation

Table 3 contains the textural and mineralogical descriptions obtained from optical petrographic analysis.

5.2.1 Sandstone texture

Textural characterization of the sandstone samples analysed in the study includes grain size, sorting and grain shape.

The grain size seen in sample LY95- 7, LY95-6-T and LY95-6-L are fine of between 0.05-0.25mm and the samples are interpreted as fine-grained sandstones that found with moderate to poor degree of sorting. Sample LY95-5 and LY95-3 were found relatively with medium to coarse-grained size ranging in between 0.17-0.55mm and with moderated sorting.

Sorting of the grains in most of the analysed samples have been observed being poor as there are mixing of grains and some rock fragments of different sizes in the sandstones analysed. Sample LY95-5 and LY95-3 were found having a moderate sorting with also some amount of porosity. Porosity is strongly related with degree of sorting; well-sorted sandstone usually has good porosity.

Shape of the grains observed in all the sample of the Battfjellet Formation under optical microscope were found being angular to sub-rounded.

5.2.2 Detrital minerals

Detrital minerals identified in the samples of the Battfjellet Formation were quartz, feldspar, mica, chert fragments and some heavy minerals (rutile, zircon and tourmaline).

Quartz

Figure 7 is dominated with the detrital quartz grains possessing angular to subangular crystal shape, these mineral grains are found in all the sandstone samples of the Battfjellet Formation. The most distinguished characteristic of the observed quartz in the polished thin section was their first order of interference colour under cross polarised light.

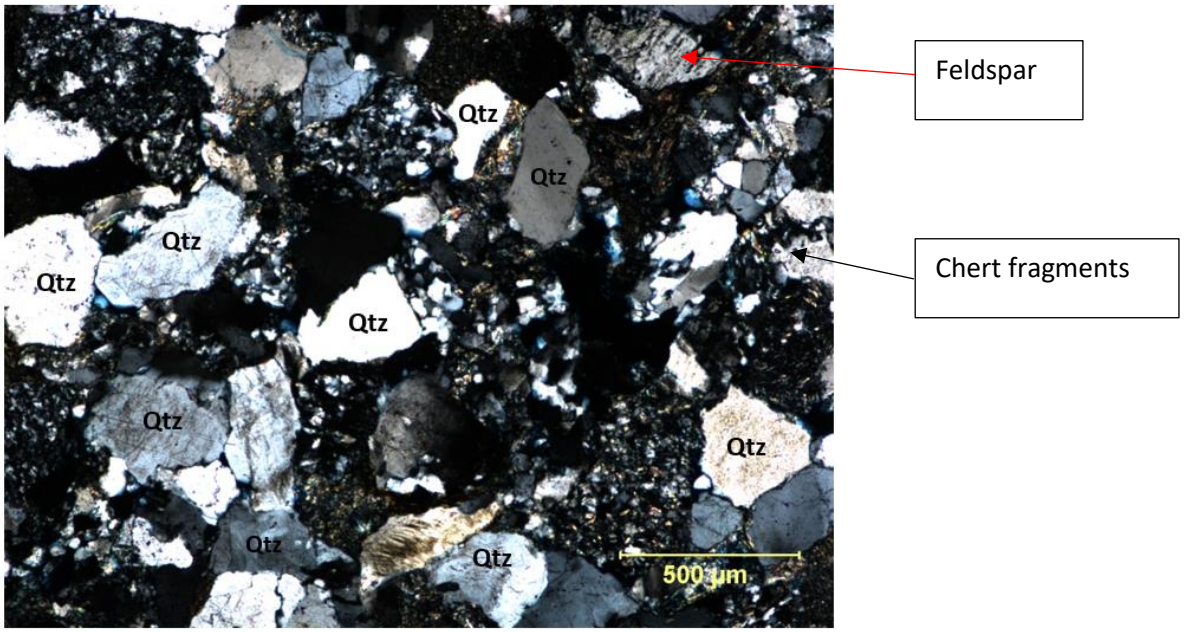

Figure 7: Detrital quartz mineral observed in a sample number LY95-5 under cross polarised light in a sample LY95-3.

Feldspar

Minor amount of feldspar minerals was observed with albite twinning under cross polarised light. The observed feldspar in Figure 8 is surrounded by detrital fragments of chert, quartz and mica.

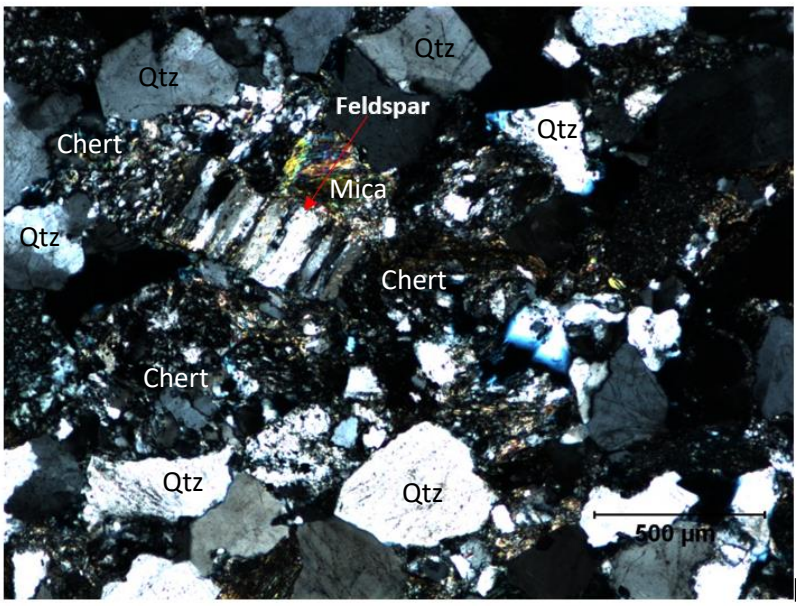

Figure 8: Detrital feldspar mineral observed under cross polarised light in the Battfjellet sandstone of the sample number LY95-3.

Mica

Figure 9 shows the detrital mica fragments that were observed in a polished thin section sample possessing a moderate to high interference colours in cross-polarised light. Both muscovite and biotite were observed, biotite was distinguished by its brown colour while muscovite was exhibiting white colour under cross polarised light. Biotite found dominating more the analysed sample comparing to muscovite. The mica mineral was observed surrounded by quartz minerals. Some of the mica fragments were observed with some deformation (bending and fractures) caused by mechanical compaction.

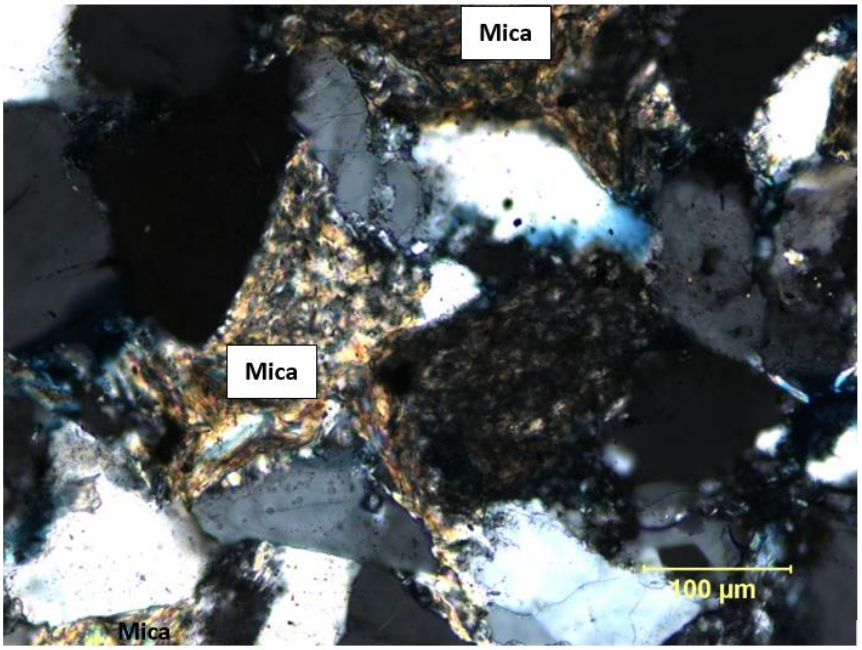

Figure 9: Micaceous fragments observed under cross polarised light in the Battfjellet sandstone of the sample number LY95-5.

Chert

Chert rock fragments (Figure 10) were also found in the studied samples as main lithic fragments in the Battfjellet Sandstone. Chert was observed composed with microcrystalline varieties of quartz.

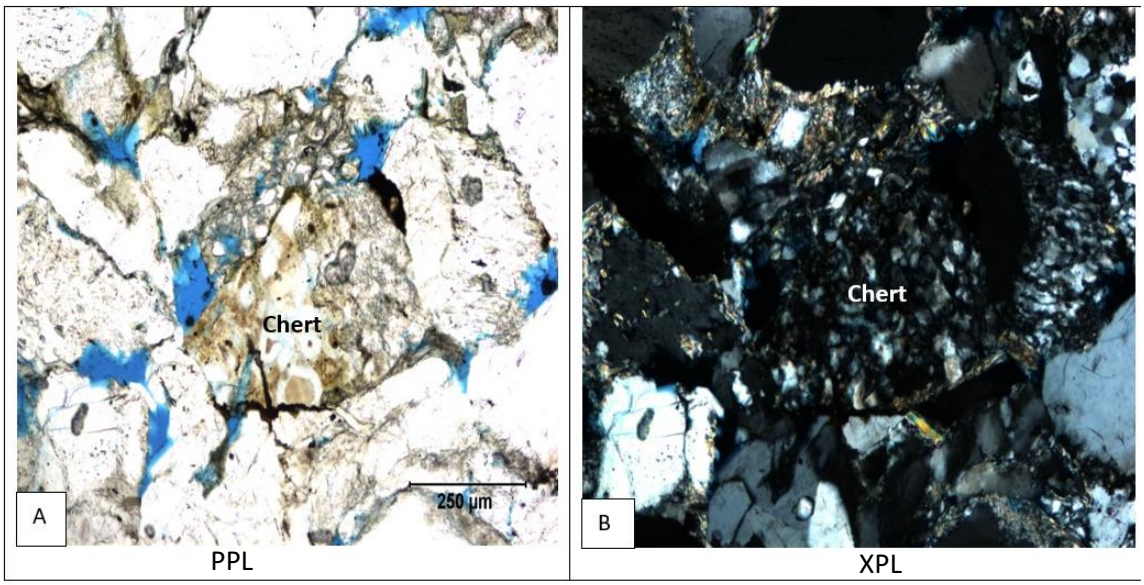

Figure 10: Chert rock fragment observed in both plane and cross polarised light in the Battfjellet Sandstone of sample number LY95-3.

Chlorite

Detrital chlorite fragment (Figure 3A) have been studied in the thin section exhibiting light green colour under plane polarised light and bluish, greyish and violet in cross polarised light. Figure 11 shows chlorite fragment that was found folded because of compaction.

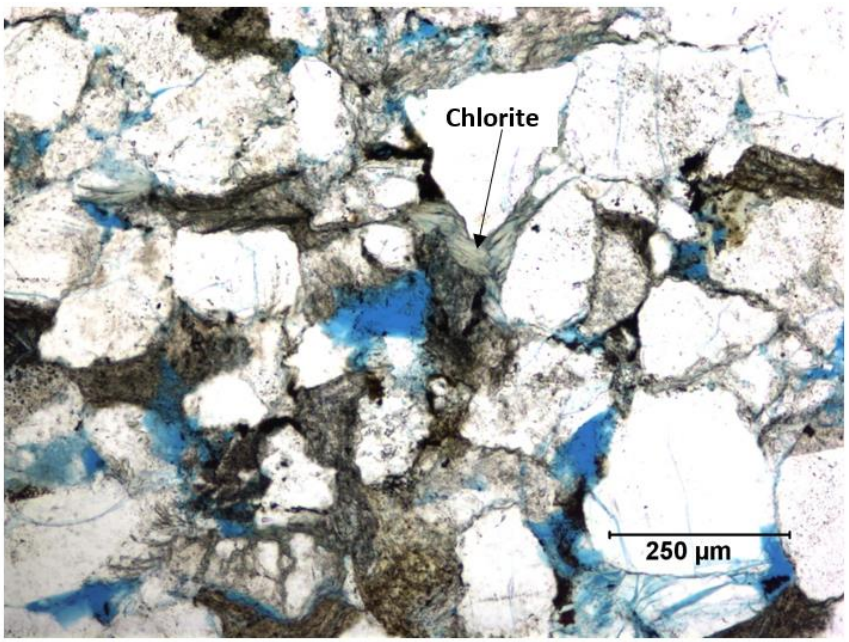

Figure 11: A deformed chlorite observed in optical photomicrography of sample number LY95-5 under plane polarised light.

Heavy minerals

The accessory heavy minerals recognised in the polished thin section sample of the Battfjellet Sandstones were rutile, zircon and tourmaline found in very small amount.

The tourmaline was found with high interference colour under cross polarised light. Also, the mineral tourmaline was observed with pale orange in plane polarised light and pinkish to purple colour under cross polarised light.

The rutile minerals found with a typically deep yellow-brown or orange-brown colour with high relief under cross polarised colour.

Zircon crystal was observed under cross polarised light possessing a red colour, with tabular prismatic shape.

5.2.3 Diagenetic minerals

The diagenetic minerals observed in the analysed sample are pyrite, siderite, calcite chalcedony and quartz.

Pyrite

Pyrite was identified by its black colour in both plane polarised and cross polarised light, the characteristic of opaque minerals as they do not transmit light under the light microscope. The cement observed filling the pores of the analysed sandstones though was observed in minor amounts. Figure 12 below shows minute crystals of authigenic pyrite mineral filling the pore spaces of the sandstone sample.

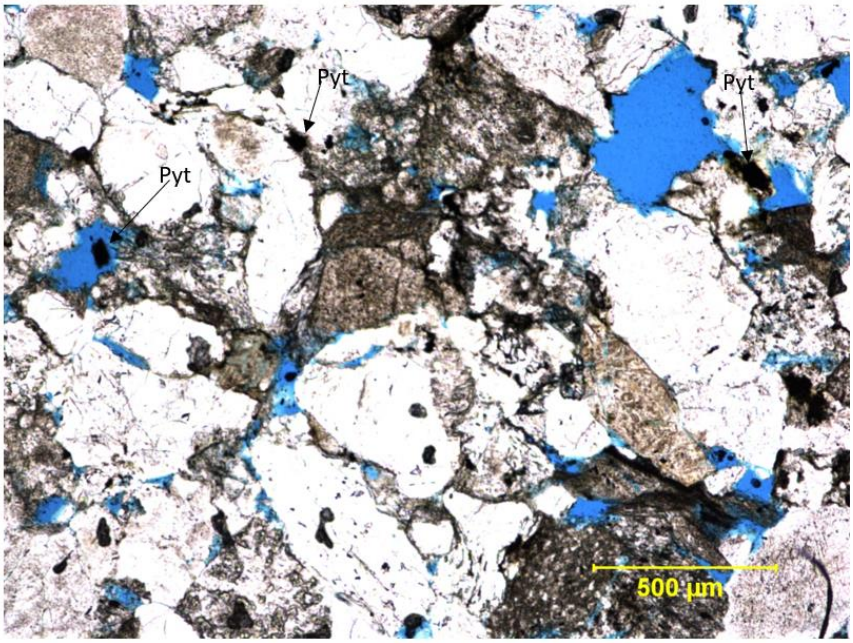

Figure 12: Diagenetic pyrite is observed in a Battfjellet Sandstone sample number LY95-3 under plane polarised light.

Calcite

The calcite cement precipitated in some of the pore spaces in the coarse-grained sandstone. The calcite cements have been observed with high interference colour showing twinning on the crystal lattice. The cement was found in the samples LY95-3 and LY95-6T from the Battfjellet Formation. The calcite cement found occurs as pore filling cement with microcrystalline texture.

Quartz cement

Quartz cement was found as overgrowth around detrital quartz grains. The cement exhibited syntaxial behaviour around quartz grain.

Chalcedony

Biogenic chalcedony showings a radial fabric structures (Figure 13), a characteristic due to fine intergrowth of silica minerals. The cement was found filling the pore spaces.

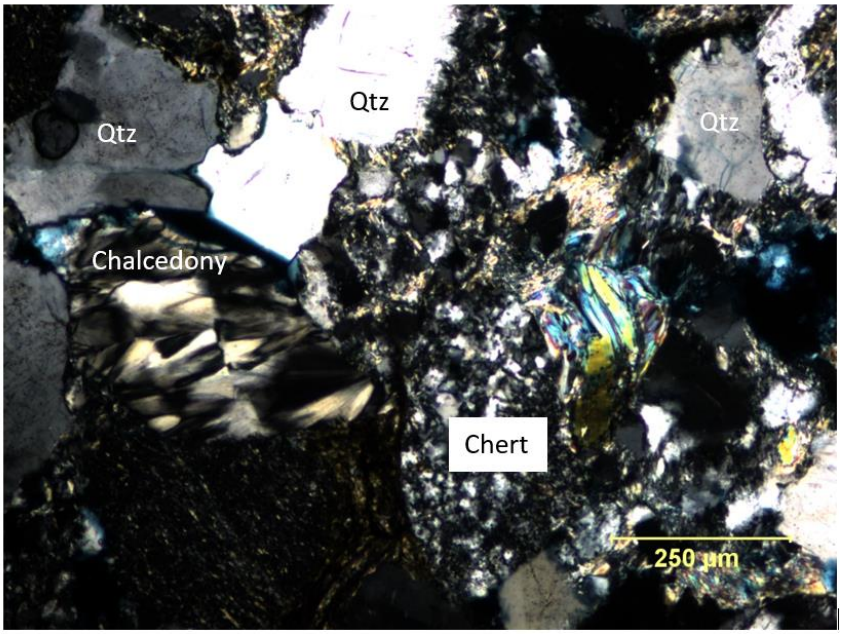

Figure 13: Chalcedony observed in a sandstone of the sample number LY95-3 under cross polarised light.

5.3 Optical petrographic results on the Aspelintoppen Formation

5.3.1 Sandstone texture

The two samples analysed from the Aspelintoppen Formation (LY95-2 and LY95-1) are fine grained ranging from 0.05mm to 0.165mm (observed under light microscope).

The grain shape observed was angular to sub-rounded as the same as what found in the Battfjellet Formation.

The degree of sorting in the two samples analysed in this formation was found being poor to moderate as the sandstone was found with the mixture of different size of grains of clay and silt size.

5.3.2 Detrital minerals

The detrital grains found in the analysed two samples from the Aspelintoppen Formation are quartz, feldspar, mica and chert fragments. The observed minerals are the same with the ones described in the Battfjellet sandstone samples. Again, quartz grains have been observed dominating all the analysed samples. Minor traces amount of feldspar was identified in the polished thin section samples. Mica rock fragments were also found in thin section sample showing the evidence of mechanical compaction due some deformation observed. Chert rock fragments have also been identified in the analysed samples. Figure 14 and Figure 15 show all the described detrital grains of the Aspelintoppen sandstones.

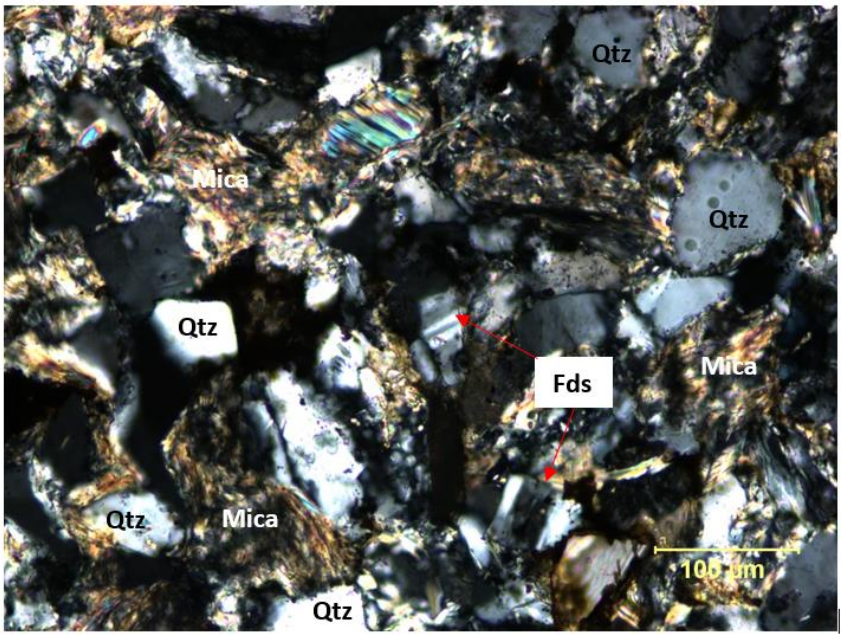

Figure 14:Quartz, mica and feldspar observed in a polished thin section sample number LY95-2 under cross polarised light.

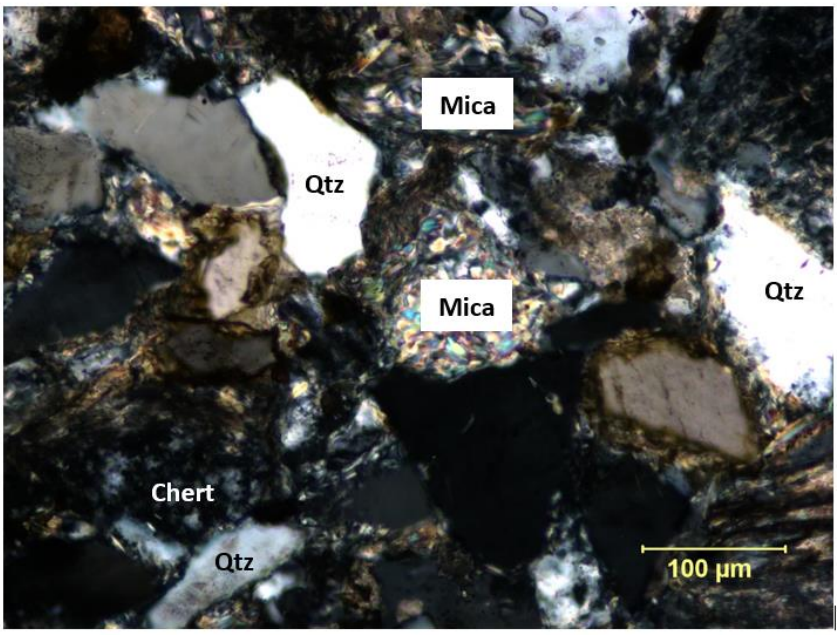

Figure 15: Chert rock fragment was observed in sample number LY95-2 under cross polarised light.

5.3.3 Diagenetic minerals

Diagenetic minerals observed in the analysed thin section samples of the Aspelintoppen Formation are siderite, carbonate and quartz cement. Both cements were found in minor trace amount filling the pore spaces of fine grained sandstone.

Carbonate cement

The carbonate cement is identified as calcite occurring as pore filling cement in the fine-grained sandstone. Calcite shows high interference colour and was observed with pale brown colour under cross polarised light. The cement was observed with twinning shown as laminations in the mineral crystal (Figure 16).

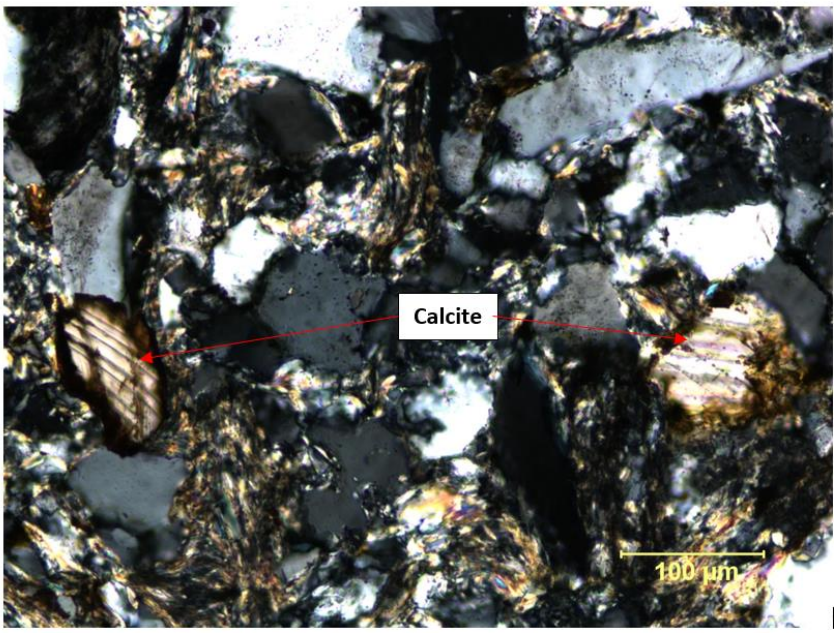

Figure 16: Authigenic calcite mineral observed in a thin section sample number LY95-2. The mineral found coated with small particles of siderite.

Siderite

Siderite was found as fine disseminated particle surrounding the detrital carbonate grains calcite (Figure 16). The cement shows brown colour as due to the presence of oxidised iron.

Quartz cement

The quartz cement was identified in the polished thin section samples of the Aspelintoppen Formation, overgrowth of quartz over the detrital quartz mineral. The cement occupies only a small part in the analysed thin section samples.

5.4 SEM petrographic results

The minerals analysed in polished thin section samples are tabulated in (Table 4). See selected EDS spectra in the Appendix. The following are the minerals identified with their texture and mineralogical descriptions.

Table 4: Mineral identification obtained from the SEM EDS analysis (see appendix)

ID number	**Chemical Fomular** (Klein, 1993)	**Mineral**	**Mode of occurance**
LY95-3_1.1	$Al_2Si2O_5(OH)_4$	Kaolinite	Diagenetic mineral
LY95-3_1.2	SiO_2	Quartz	Detrital mineral
LY95-3_1.3	$Al_2Si2O_5(OH)_4$	Kaolinite	Diagenetic mineral
LY95-3_1.4	$Al_2Si2O_5(OH)_4$	Kaolinite	Diagenetic mineral
LY95-3_1.5	SiO_2	Quartz	Detrital mineral
LY95-3_1.6	SiO_2	Quartz	Detrital mineral
LY95-3_1.7	SiO_2	Quartz	Detrital mineral
LY95-3_1.8	$(Mg,Fe)_3(Si,Al)_4O_{10}$	Chlorite	Diagenetic mineral
LY95-3_1.9	$Al_2Si2O_5(OH)_4$	Kaolinite	Diagenetic mineral
LY95-3_1.10	$(Mg,Fe)_3(Si,Al)_4O_{10}$	Chlorite	Diagenetic mineral
LY95-3_1.11	$FeCO_3$	Siderite	Diagenetic mineral
LY95-3_1.12	$KAlSi_3O_8$	K-feldspar	Detrital mineral
LY95-3_1.13	$KAlSi3O_8$	K-feldspar	Detrital mineral
LY95-3_1.14	$NaAlSi_3O_8$	Albite	Detrital mineral
LY95-3_1.15	$NaAlSi_3O_8$	Albite	Detrital mineral
LY95-3_1.16	$KAlSi_3O_8$	K-feldspar	Detrital mineral
LY95-3_1.17	$(Mg,Fe)_3(Si,Al)_4O_{10}$	Chlorite	Diagenetic mineral

LY95-3_1.18	$(Mg,Fe)_3(Si,Al)_4O_{10}$	Chlorite	Diagenetic mineral
LY95-3_1.19	$(Mg,Fe)_3(Si,Al)_4O_{1o}$	Chlorite	Diagenetic mineral
LY95-3_1.20	SiO_2	Quartz	Detrital mineral
LY95-3_1.21	$KAl_3Si_3O_{10}(OH)_2$	Muscovite	Detrital mineral
LY95-3_1.22	$(Mg,Fe)_3(Si,Al)_4O_{10}$	Chlorite	Detrital mineral
LY95-3_1.23	TiO_2	Rutile	Detrital mineral
LY95-3_1.24		Mixed analysis	
LY95-3_1.25	$NaAlSi_3O_8$	Albite	Detrital mineral
LY95-3_1.26	$KAlSi_3O_8$	K-Feldspar	Detrital mineral
LY95-3_1.27	SiO_2	Quartz	Detrital mineral
LY95-3_1.28	SiO_2	Quartz	Detrital mineral
LY95-3_1.29	$K(Mg,Fe)_3(AlSi_3O_{10})(F,OH)_2$	Biotite	Detrital mineral
LY95-3_1.30	SiO_2	Quartz	Detrital mineral
LY95-3_1.31	$(Mg,Fe)_3(Si,Al)_4O_{1o}$	Chlorite	Diagenetic mineral
LY95-3_1.32	$(Mg,Fe)_3(Si,Al)_4O_{1o}$	Chlorite	Diagenetic mineral
LY95-3_1.33	SiO_2	Quartz	Detrital mineral
LY95-3_1.34	SiO_2	Chert	Detrital mineral
LY95-3_1.35	$(Mg,Fe)_3(Si,Al)_4O_{1o}$	Chlorite	Diagenetic mineral
LY95-3_1.36	SiO_2	Quartz	Detrital mineral
LY95-5_1.1	SiO_2	Quartz	Detrital mineral
LY95-5_1.2	SiO_2	Quartz	Detrital mineral
LY95-5_1.4	$FeCO_3$	Siderite	Diagenetic mineral
LY95-5_1.5	SiO_2	Quartz	Detrital mineral

LY95-5_1.6	SiO_2	Quartz	Detrital mineral
LY95-5_1.7	$K(Mg,Fe)_3(AlSi_3O_{10})(F,OH)_2$	Biotite	Detrital grain
LY95-5_1.8	$(Mg,Fe)_3(Si,Al)_4O_{1o}$	Chlorite	Detrital grain
LY95-5_1.9	$K(Mg,Fe)_3(AlSi_3O_{10})(F,OH)_2$	Biotite	Detrital grain
LY95-5_1.10	SiO_2	Quartz	Detrital mineral
LY95-5_1.11	$(Mg,Fe)_3(Si,Al)_4O_{1o}$	Chlorite	Detrital grain
LY95-5_1.12	TiO_2	Rutile	Detrital mineral
LY95-5_1.13	$(Mg,Fe)_3(Si,Al)_4O_{1o}$	Chlorite	Detrital grain
LY95-5_1.14	$(Mg,Fe)_3(Si,Al)_4O_{1o}$	Chlorite	Detrital grain
LY95-5_1.15		Mixed Siderite	Detrital grains
LY95-5_1.16	$K(Mg,Fe)_3(AlSi_3O_{10})(F,OH)_2$	Biotite	Detrital grain
LY95-5_1.17	$(Mg,Fe)_3(Si,Al)_4O_{1o}$	Chlorite	Detrital grain
LY95-5_1.18	SiO_2	Quartz	Detrital mineral
LY95-5_1.19	$K(Mg,Fe)_3(AlSi_3O_{10})(F,OH)_2$	Biotite	Detrital grain
LY95-5_1.20	$Al_2Si2O_5(OH)_4$	Kaolinite	Diagenetic mineral
LY95-5_1.21	$Al_2Si2O_5(OH)_4$	Kaolinite	Diagenetic mineral
LY95-5_1.22	$(Mg,Fe)_3(Si,Al)_4O_{1o}$	Chlorite	Diagenetic mineral
LY95-5_1.23	SiO_2	Quartz	Detrital mineral
LY95-5_1.24	SiO_2	Chert	Detrital mineral
LY95-5_1.25	SiO_2	Quartz	Detrital mineral
LY95-5_1.26	SiO_2	Quartz	Diagenetic mineral
LY95-5_1.27	SiO_2	Quartz	Detrital mineral

LY95-5_1.28	SiO_2	Chert	Detrital grain
LY95-5_1.29	SiO_2	Quartz	Detrital mineral
LY95-5_1.30	SiO_2	Quartz	Detrital mineral
LY95-5_1.31	SiO_2	Quartz	Detrital mineral
LY95-5_1.32	SiO_2	Quartz	Diagenetic mineral
LY95-5_1.33	$FeCO_3$	Siderite	Detrital grain
LY95-5_1.34	FeS	Pyrite	Diagenetic mineral
LY95-5_1.35	$(Mg,Fe)_3(Si,Al)_4O_{1o}$	Chlorite	Diagenetic mineral
LY95-5_1.36	SiO_2	Quartz	Detrital mineral
LY95-5_1.37	FeS	Pyrite	Diagenetic mineral
LY95-5_1.38	SiO_2	Chert	Detrital mineral
LY95-5_1.39	$FeCO_3$	Siderite	Diagenetic mineral
LY95-5_1.40	$K(Mg,Fe)_3(AlSi_3O_{10})(F,OH)_2$	Biotite	Detrital grain
LY95-5_1.41	$KAlSi_3O_8$	K-Felspar	Detrital mineral
LY95-5_1.42	$(Mg,Fe)_3(Si,Al)_4O_{1o}$	Chlorite	Diagenetic mineral
LY95-5_1.43	$(Mg,Fe)_3(Si,Al)_4O_{1o}$	Chlorite	Diagenetic mineral
LY95-5_1.44	$K(Mg,Fe)_3(AlSi_3O_{10})(F,OH)_2$	Biotite	Detrital grain
LY95-5_1.45	$(Mg,Fe)_3(Si,Al)_4O_{1o}$	Chlorite	Diagenetic mineral
LY95-6L_1	$ZrSiO_4$	Ziricon	Detrital mineral
LY95-6L_2	$(Mg,Fe)_3(Si,Al)_4O_{1o}$	Chlorite	Diagenetic mineral
LY95-6L_3	$NaAlSi_3O_8$	Albite	Detrital mineral
LY95-6L_4	$NaAlSi_3O_8$	Albite	Detrital mineral
LY95-6L_5	$K(Mg,Fe)_3(AlSi_3O_{10})(F,OH)_2$	Biotite	Detrital grain

LY95-6L_6	$CaCO_3$	Calcite	Diagenetic mineral
LY95-6L_7	$FeCO_3$	Siderite	Diagenetic mineral
LY95-6L_8	$FeCO_3$	Siderite	Diagenetic mineral
LY95-6L_9	SiO_2	Quartz	Detrital mineral
LY95-6L_10	$CaCO_3$	Calcite	Diagenetic mineral
LY95-6L_11	$FeCO_3$	Siderite	Diagenetic mineral
LY95-6L_12	$K(Na,Ca)Al_{1.3}Fe_{0.4}Mn_{0.2}Si_{3.4}Al_{0.6}O_{10}(OH)_2$	Illite	Diagenetic mineral
LY95-6L_13	$K(Na,Ca)Al_{1.3}Fe_{0.4}Mn_{0.2}Si_{3.4}Al_{0.6}O_{10}(OH)_2$	Illite	Diagenetic mineral
LY95-6L_14	$NaAlSi_3O_8$	Albite	Detrital mineral
LY95-6L_15	$Al_2Si2O_5(OH)_4$	Kaolinite	Diagenetic mineral
LY95-6L_16	SiO_2	Quartz	Detrital mineral
LY95-6L_17	$Ca_2(Al,Fe)_2(SiO_4)_3(OH)$	Epidote	Detrital mineral
LY95-6L_18	$K(Mg,Fe)_3(AlSi_3O_{10})(F,OH)_2$	Biotite	Detrital grain
LY95-6L_20	$(Mg,Fe)_3(Si,Al)_4O_{1o}$	Chlorite	Detrital grain
LY95-6L_21	SiO_2	Quartz	Detrital mineral
LY95-6L_22	SiO_2	Quartz	Detrital mineral
LY95-6L_23	$(Mg,Fe)_3(Si,Al)_4O_{1o}$	Chlorite	Detrital grain
LY95-6L_24	$(Mg,Fe)_3(Si,Al)_4O_{1o}$	Chlorite	Detrital grain
LY95-6L_25	$Al_2Si2O_5(OH)_4$	Kaolinite	Diagenetic mineral
LY95-6L_26	SiO_2	Chert	Detrital grain
LY95-6L_27		Mixed elements	
LY95-6L_28	$K(Mg,Fe)_3(AlSi_3O_{10})(F,OH)_2$	Biotite	Detrital grain
LY95-6L_29	$CaCO_3$	Calcite	Diagenetic mineral

LY95-6L_30	$Al_2Si2O_5(OH)_4$	Kaolinite	Diagenetic mineral
LY95-6L_31	$FeCO_3$	Siderite	Diagenetic mineral
LY95-6L_32	$FeCO_3$	Siderite	Diagenetic mineral
LY95-6L_33	$FeCO_3$	Siderite	Diagenetic mineral
LY95-6L_34	$Al_2Si2O_5(OH)_4$	Kaolinite	Diagenetic mineral
LY95-6L_35	$NaAlSi_3O_8$	Albite	Detrital mineral
LY95-6L_36	SiO_2	Chert	Detrital mineral
LY95-6L_37	SiO_2	Quartz	Detrital mineral
LY95-6L_38	$Ca_2(Fe,Al)Al_2(SiO_4)(Si_2O_7)O(OH)$	Epidote	Detrital grain
LY95-6L_39	SiO_2	Quartz	Detrital mineral
LY95-6L_40	$NaAlSi_3O_8$	Albite	Detrital mineral
LY95-6L_41	SiO_2	Quartz	Detrital mineral
LY95-6L_43	$K(Na,Ca)Al_{1.3}Fe_{0.4}Mn_{0.2}Si_{3.4}Al_{0.6}O_{10}(OH)_2$	Illite	Diagenetic mineral
LY95-6L_44		Coal	Detrital grain
LY95-6L_45	$NaAlSi_3O_8$	Albite	Detrital mineral
LY95-6L_47	$(Mg,Fe)_3(Si,Al)_4O_{1o}$	Chlorite	Detrital grain
LY95-6L_48	SiO_2	Quartz	Detrital mineral
LY95-6L_49	$Al_2Si2O_5(OH)_4$	Kaolinite	Diagenetic mineral
LY95-6L_50	SiO_2	Quartz	Detrital mineral

5.4.1 Detrital minerals

The detrital minerals that have been identified by scanning electron microscopy in the samples from the Battfjellet Formation were quartz, K-feldspar, albite, zircon, rutile, epidote, muscovite, biotite, and chert fragments.

Quartz

Quartz grains are the dominant detrital minerals identified in all sandstones sample of the Battfjellet Formation displayed with grey colour in BEI (Figure 17). The identification of this mineral was done with the aid of the EDS which contains the elemental composition of the identified mineral (Appendix, Figure 35). Quartz has been identified occurring as monocrystalline grains with sub angular to sub rounded shape.

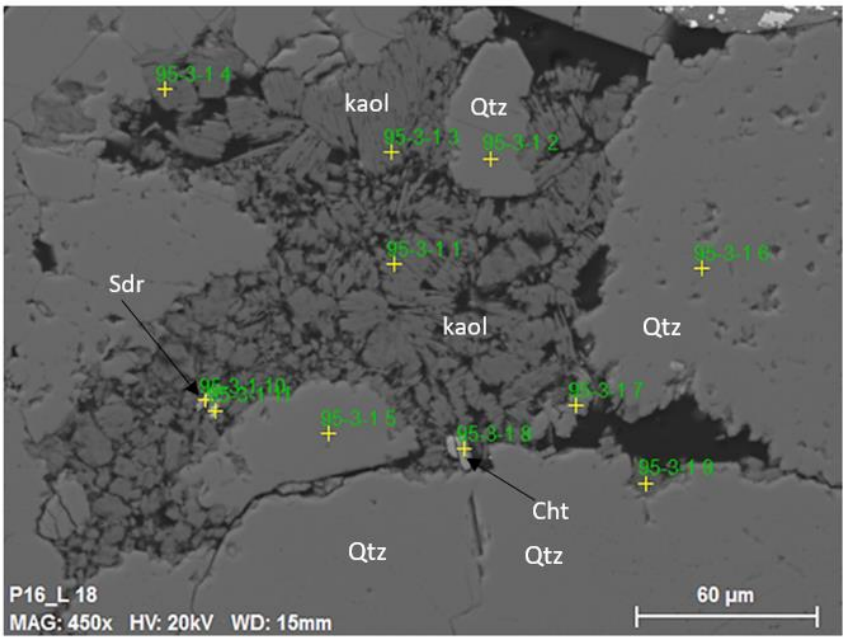

Figure 17: Backscattered Electron image showing quartz grains dominating the thin section sample number LY95-3. Kaolinite is identified occurring as pore filling authigenic cement.

Mica

The mica minerals (biotite and muscovite) have been identified in the analysed thin section samples. Biotite minerals are the most dominate grains found in most of all samples of the

Battfjellet Formation, it was identified with lighter grey colour as compared to the colour of quartz in a BEI (Figure 18). The EDS analysis helped on identifying the biotite mineral (Appendix, Figure 34) showing the major elements that are composed in the mineral. The bending fold structures were identified on the biotite observed.

Muscovite have been found in small patches observed occurring adjacent quartz (Figure 22), it has a lighter grey colour as compared to biotite. It was found in very small amount in the analysed sample. The EDS analysis contributed much on recognising this mineral in a Backscattered Electron image (Appendix, Figure 37).

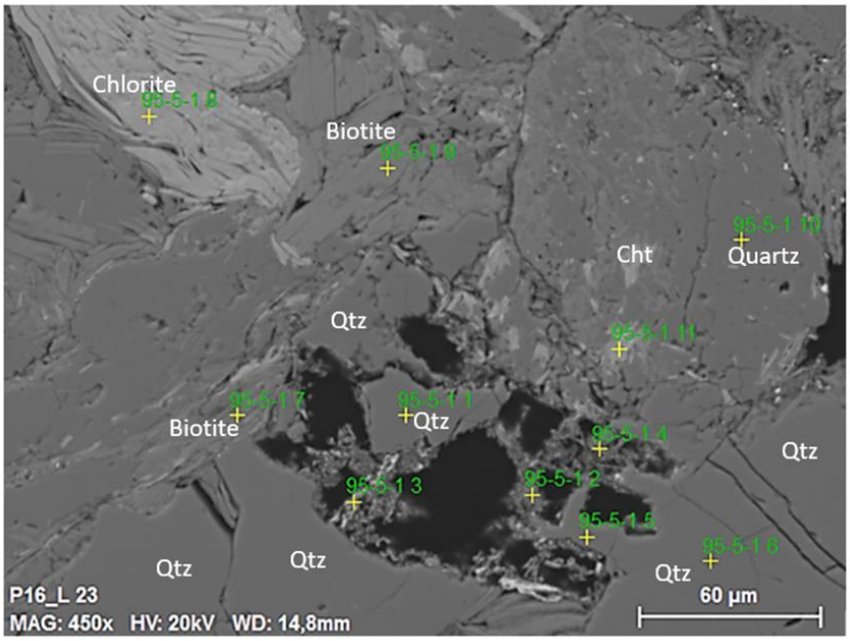

Figure 18: The deformed detrital biotite and chlorite minerals examined on upper left part of BEI in the sample LY95-5. Secondary porosity is seen in the lower part of the image.

Feldspar

The observed feldspar in these samples were albite and K-feldspar. In generals these minerals were only found in very small amount in the analysed thin section samples. Albite was observed having a dark grey colour while K-feldspar was found with lighter grey colour. Albite is observed occurring adjacent to K-feldspar (Figure 19). Electron dispersive spectral which is found in Appendix (Figure 39 and Figure 40) shows elemental composition of the describe feldspar minerals.

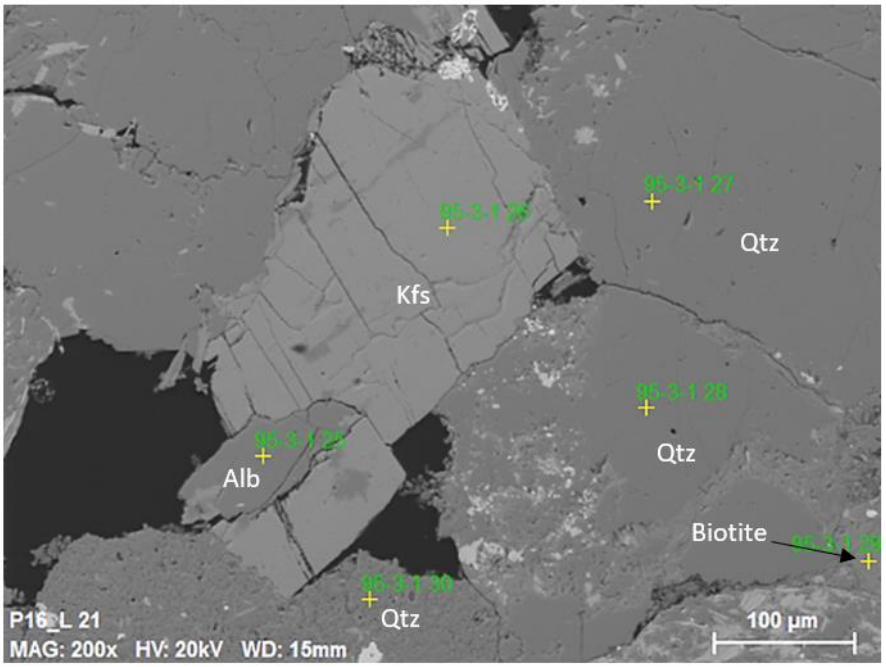

Figure 19: A SEM BEI with K-feldspar and albite minerals in sample number LY95-3.

Heavy minerals

Rutile (Figure 22 and Figure 23) and zircon (Figure 20) observed in BEI with light colour that is caused with their high density. Energy Dispersive Spectral was the key factor used on identifying the minerals as the elemental composition of each mineral were studied (Figure 38 and Figure 44). These minerals were found in very small amount in the observed samples of the Battfjellet Sandstones.

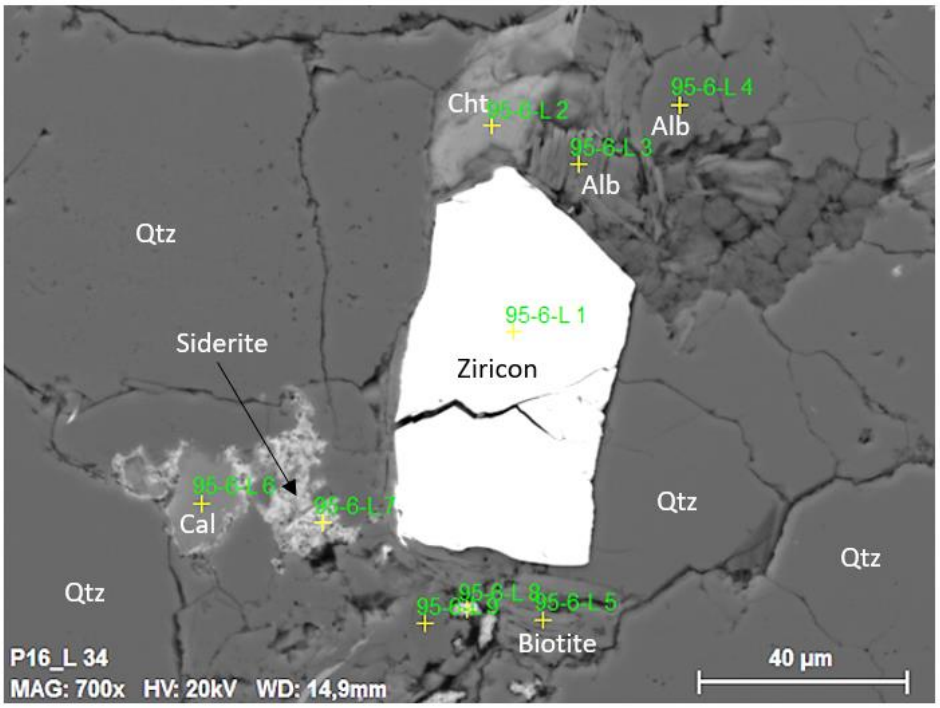

Figure 20: BEI micrography with zircon mineral having a light colour in sample LY95-6L.

Chert

Chert rock fragments were found dominating most of the analysed samples. In BEI chert were found with grey colour like the identified colour of quartz but observed with micro pores all around the rock fragment (Figure 21). The chert rock fragments have been found in all analysed samples of the Battfjellet sandstone. EDS shows the same elemental composition as that of the quartz mineral.

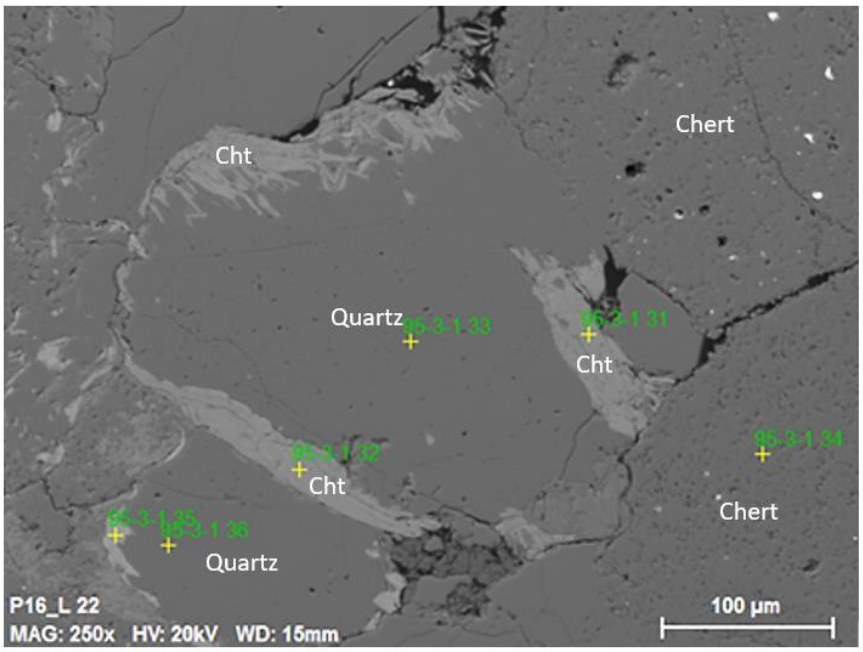

Figure 21: A BEI with detrital chert rock fragments surrounded with quartz minerals in sample LY95-3.

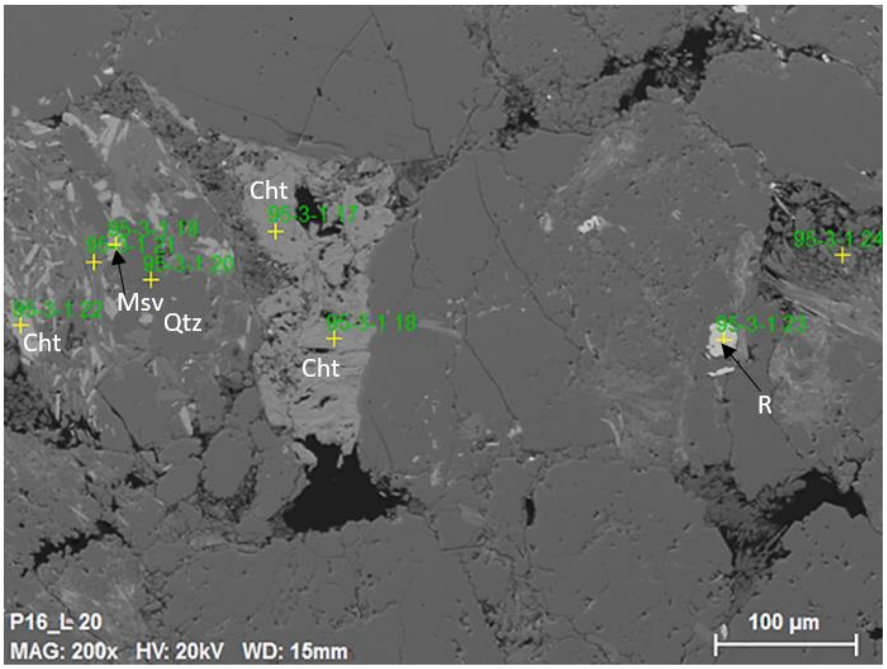

Figure 22: A BEI showing mineral chlorite alteration replacing the grain of quartz on the left part of the image. rutile and muscovite are also observed in BEI of sample LY95-3.

Detrital chlorite

The detrital chlorite fragment has been studied in the BEI exhibiting a lighter grey colour. The mineral was found with bending structure which is the evidence of mechanical compaction (Figure 18 and Figure 23). EDS analysis that was used on identification of this mineral is displayed in Appendix (Figure 36)

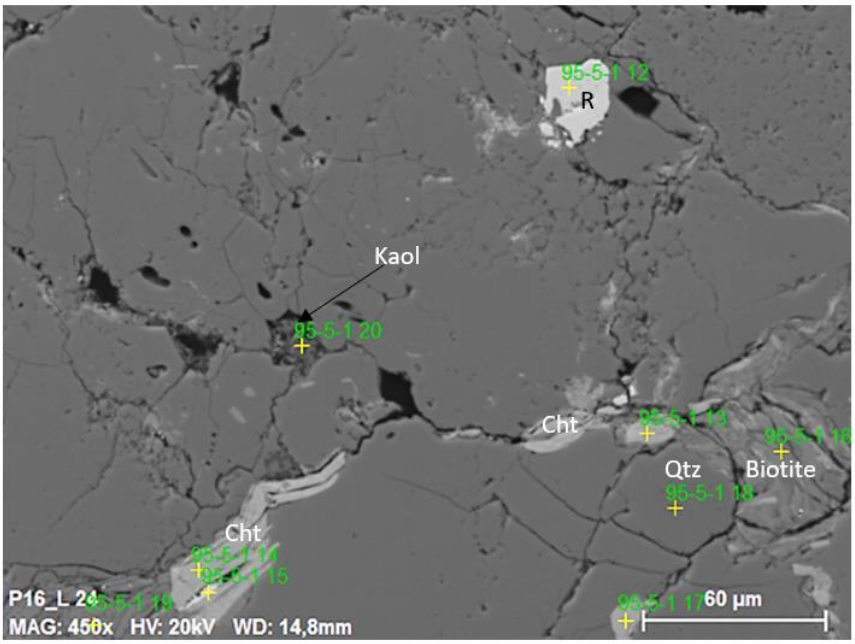

Figure 23:A BEI with bended detrital chlorite. The rutile mineral is observed surrounded with grains of quartz and chert rock fragments in sample LY95-5

Epidote

Epidote observed in thin section sample number LY95-6L of Battfjellet Formation, it is exhibiting some bending structure with some fractures that are filled with quartz (Figure 24). The EDS analysis shows the epidote mineral being composed with some magnesium and manganese content as what is displayed in Appendix (Figure 43).

Detrital coal fragment was also observed in this sample and was found occurring adjacent to epidote mineral. It was observed with black colour which is caused with the low weight possessed with this fragment. Some fractures have been also observed in the coal fragment.

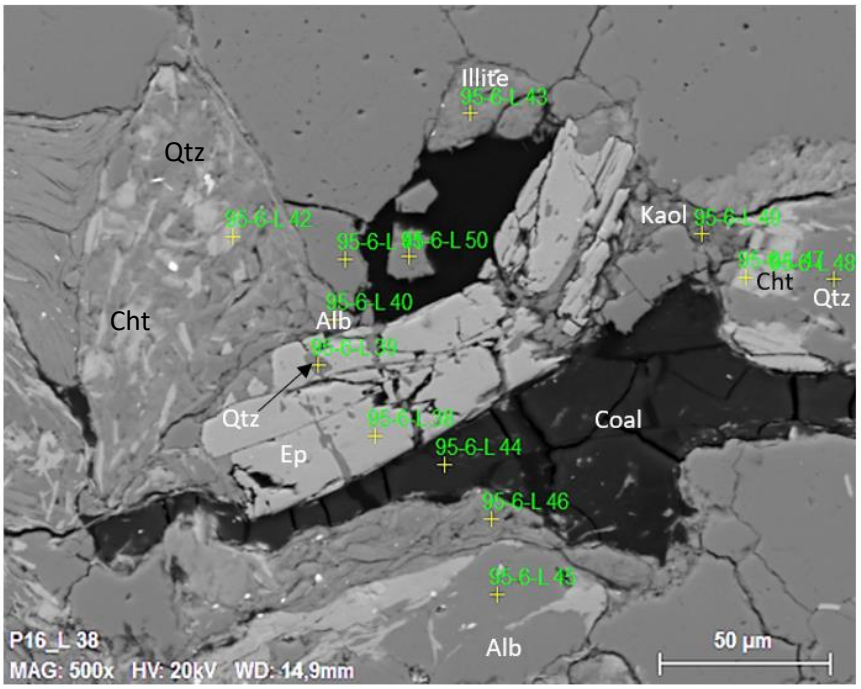

Figure 24: A BEI with fractured epidote mineral and coal fragment. Chlorite observed replacing grain of quartz mineral. Illite clay mineral occur as pore filling mineral in sample LY95-6L.

5.4.2 Diagenetic minerals

The diagenetic minerals observed in the analysed sample are pyrite, siderite, kaolinite, calcite, quartz, illite and chlorite. The following are the descriptions of the diagenetic minerals observed.

Pyrite and siderite

Pyrite was observed as small patches of crystals filling the porous chert fragments and some found in pore spaces between the mineral grains. Pyrite is a heavy mineral which is displayed with bright white colour in BEI (Figure 25). Some of the pyrite minerals were observed in pore spaces between mineral grains. The EDS analysis prove the observed particle being pyrite as it shows the typical element composition of the mineral (Appendix, Figure 42).

Siderite was also found as pore filling cement in most of the sandstone samples of the Battfjellet Formation (Figure 25). The EDS shows siderite observed being composed with other elements in addition to the iron such as magnesium, silicon and manganese as shown in Appendix (Figure 41). Silicon is considered as impurity, whereas magnesium and manganese are common elements found in siderite.

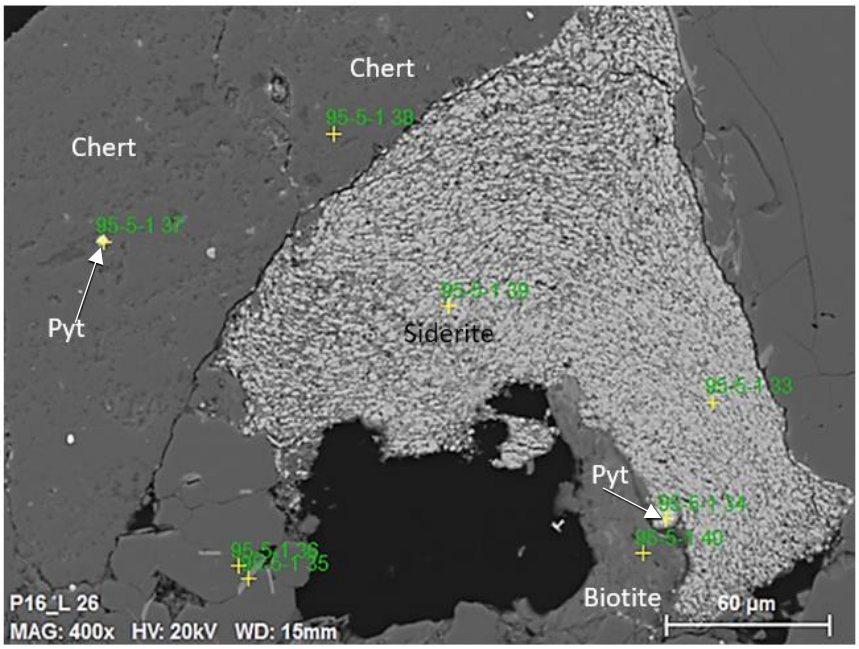

Figure 25: Pyrite occurs as pore filling in a pore spaces that are found in chert, siderite is also found as the pore filling authigenic mineral in a thin section sample LY95-5.

Calcite

The calcite cement found occuring as pore filling cement with microcrystalline texture. The cement was identified by studying the elements composed in EDS (Appendix, Figure 45). The cement was recognised with light grey colour surrounded by crystal of siderite mineral (Figure 26 and Figure 28). The cement was found not dominating much the analysed sample of the Battfjellet Sandstones.

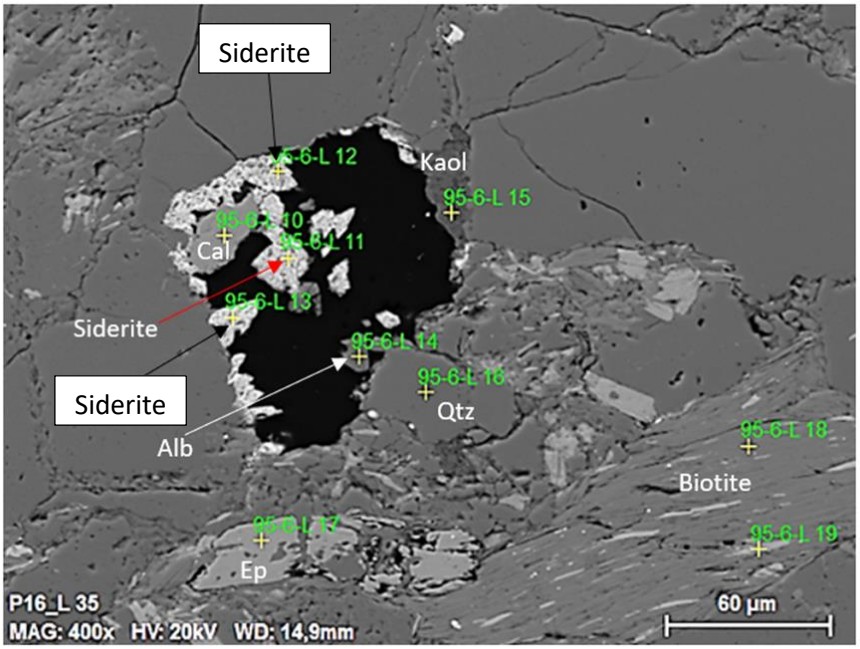

Figure 26: Illite, siderite, albite, biotite, kaolinite, quartz and epidote minerals in sample LY95-6L. Small minute crystals of illite are found filling the siderite mineral.

Quartz cement

Figure 27 shows well-developed crystals of quartz mineral that were identified in some pore spaces of the Battfjellet Sandstones. The diagenetic quartz was found in the pore spaces of the sample number LY95-5, their occurrence in the sandstones has to do with the reduction of the pore spaces as they occur as pore filling minerals.

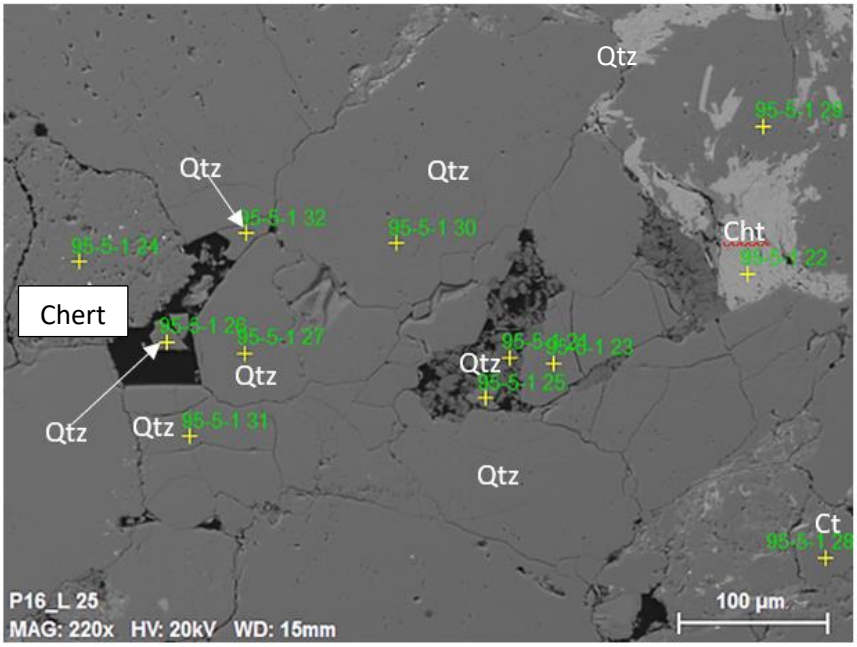

Figure 27: Microcrystalline quartz minerals filling the pore spaces in the Battfjellet Sandstone of sample LY95-5.

Clay minerals

Phyllosilicate clay minerals observed in sandstone of the Battfjellet Formation are kaolinite, illite and chlorite. Most of the observed clay occur as pore filling minerals, and some clays were found replacing the detrital grains. The clay minerals were easily identified in the SEM analysis with the aid of BEI and EDS. Here are the descriptions of clay minerals observed in the analysed thin section sample.

Kaolinite

Kaolinite clay mineral was identified as pore filling mineral under BEI. Most of the sandstone sample presenting the Battfjellet Formation were found dominated by kaolinite in their open spaces. The mineral has characteristic of dark grey colour as shown in Figure 17 and Figure 28. The EDS analysis shows the elements available in this clay mineral (Appendix, Figure 47)

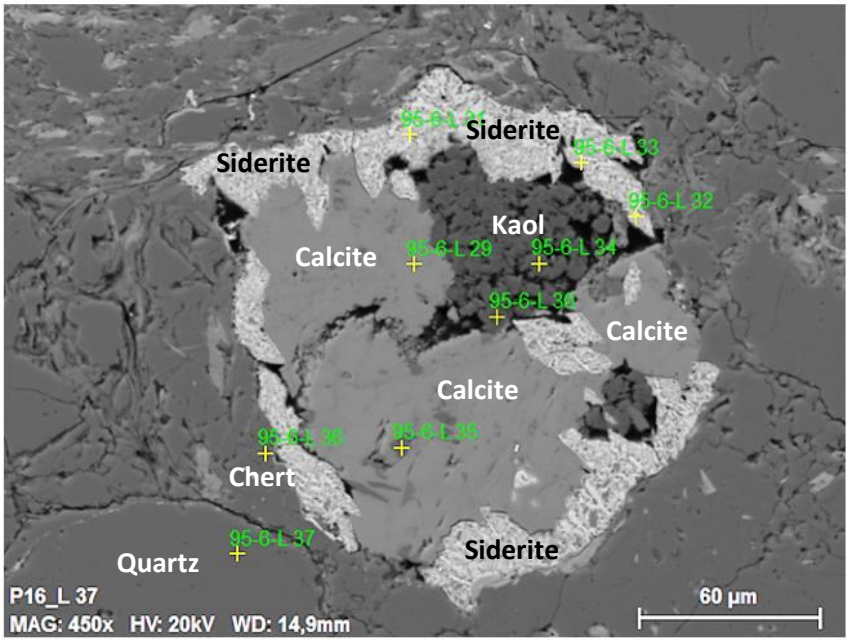

Figure 28: Kaolinite, siderite and calcite observed occurring as pore filling mineral in sample number LY95-6L.

Chlorite

The crystals of chlorite mineral were observed dominating most of the analysed sample occurring as pore filling authigenic minerals (Figure 29). Chlorite was found with lighter grey colour with EDS showing all the important available elements (Appendix, Figure 46). Some of the chlorite were found as replacive mineral in the grains of quartz (Figure 24 and Figure 33).

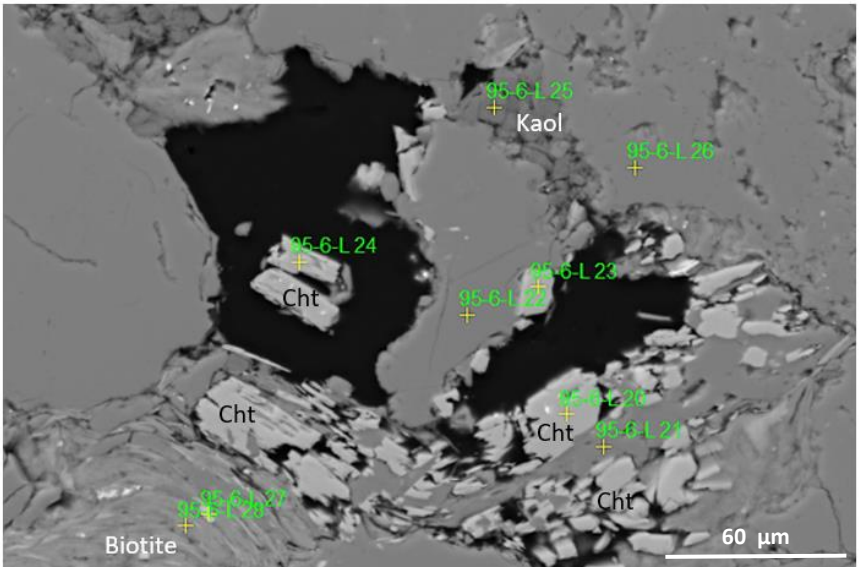

Figure 29: Chlorite and kaolinite occur as pore filling mineral, deformed biotite observed in the analysed sandstone sample LY95-6L.

Illite

The illite clay mineral was observed in a very small amounts in the analysed sandstone samples of the Battfjellet Formation. It was observed with dark grey colour in BEI. The EDS analysis shows the elemental composition of illite as it was the main tool used on identifying this mineral (Apendix, Figure 48). This mineral was found as pore filling mineral (Figure 24) and some were observe occurring nearby siderite mineral (Figure 26).

6. DISCUSSION

This chapter discuss the results obtained from petrographic studies and imagej porosity analysis. The discussion will cover on sandstone maturity, provenances, mechanical compaction and the origin and impacts of authigenic minerals with relation to quality of the reservoir.

6.1 Sandstone Maturity

Sandstones from Battfjellet Formation were found composed with quartz, albite, K-feldspar, chlorite, epidote, zircon, rutile, chert, biotite, muscovite and epidote. The sandstone compositions and amount of lithic rock fragments indicates the sandstone is mineralogical immature. The sandstones are categorised as textural immature as it is found with angular grains and with moderate to poor sorting same as the models by (Folk, 1951).

The same findings were found in the sandstones of the Aspelintoppen Formation that these sandstones are mineralogical and textural immature. Helland-Hansen (1990) described the Paleogene sandstones of the foreland basin of Spitsbergen being texturally immature suggesting the source of sediments was not far away as the sandstones were found composed with unstable rock fragments of shale and slate clasts. It also supported by the presence of sub angular to angular mineral grains that are characterising the mineral grains of the sandstones from the Aspelintoppen Formation, the angularity of mineral grains shows the sediments were transported in short distance as they are found possessing their original shapes obtained during weathering (Beard & Weyl, 1973).

The mineralogical composition that was identified in this study looks like the one found with Helland-Hensan (2010). His study has contributed much to the knowledge concerning petrography study of the Battfjellet Formation in Nordenskiöld Land (Figure 1). The study concluded that the Battfjellet Formation is composed of quartz and rock fragments of 40% and 50% respectively, with minor amount of 5% feldspar and 4% of carbonaceous detritus. More of his findings has been summarised on previous studies which is found in chapter 1 of this report.

6.2 Provenance

The deposited sediments in Nordenskiöld Land has been interpreted to have originated from the west Spitsbergen thrust belt (Helland-Hansen, 1990). The thrust belt is characterised with sedimentary and metamorphic rocks. Below are some of the minerals that are found in the analysed sandstones supporting that the provenance of the sediments are from igneous, metamorphic and sedimentary terrains.

Biotite is very common in a variety of igneous and metamorphic rocks. In igneous rocks, it is found more commonly in silicic and alkalic rocks. It also found in immature sedimentary rocks but will change to clay minerals when weathered. The presence of biotite mineral in the analysed sandstones shows that the sediments were derived from metamorphic and sedimentary provenances.

Rutile is a common accessory mineral that is most found in high temperature and pressure rocks originated from metamorphic and igneous rocks. The observed mineral was found in very low amount and its presence in the analysed sandstones indicates the sediments were derived from metamorphic and igneous area.

Zircon is a common accessory trace mineral constituent of most felsic igneous rocks such as granite and diorite. It is most found in most of sedimentary rocks as it is very resistance to abrasion during transportation to the sedimentary basin. It is also chemically stable as it does not react with other minerals (Wilde, et al., 2001). The availability of zircon in the analysed sandstone prove some of the sediments were derived from igneous terrain, or from reworked sedimentary deposits.

The presence of epidote in the Battfjellet Sandstones shows that the sediments were derived from metamorphic source area as it is most found in marble and schistose rocks of metamorphic origin, or igneous areas that are relating to hydrothermal alteration of various minerals of such as feldspars, micas, pyroxenes, amphiboles and garnets (Apted & Liou, 1983).

Biogenic chert mineral is common in the underlying Palaeozoic sedimentary rocks found in Spitsbergen, Svalbard, they were formed in Permian Chert Event during the period of warm temperature (Worsley, 2008). They are also found in limestone and dolomite that are characterised with fragment of brachiopods (Brachiopod Chert) formed in Permian (Gobbett, 1963). The available chert fragments in the analysed sandstones show that they might have been originated from the underlying Palaeozoic sedimentary rocks of Spitsbergen, Svalbard.

6.3 Mechanical Compaction

Mechanical compaction lead to volume reduction in a compacted rock as the compacted rock attains a densely packed mineral grain. Usually mechanical compaction involves rearrangement of mineral grains, formation of pseudomatrix, mechanical fracturing and removal of pore water. It is caused by the increasing of overburden weight in already deposited sediments in a sedimentary basin (Worden & Burley, 2003).

Most of the analysed samples have been found with the evidence of compaction, such evidence includes bended and deformed detrital rock fragments. The major effects of compaction are loss of porosity, reduction in sedimentary thickness and increase of bulk density (Allen & Allen, 2013). Mechanical compaction is the main reason for porosity loss in sandstones found in the Battfjellet and Aspelintoppen formations. Most of the analysed thin section samples from these formations were observed containing ductile rock fragments that were easily deformed during compaction. As it has been reported by Mansurbeg, et al. (2013) that mechanical compaction was the main reason for porosity loss on the analysed sandstones of the Eocene Central Basin in Spitsbergen.

The evidence for mechanical compaction can be observed on the biotite and detrital chlorite (Figure 23) that are showing flexural shapes and some minerals flakes were even found fractured due to the encountered intense compaction.

Other deformed minerals are the metamorphic rock fragments such as micaceous rock fragments, that were easily deformed during mechanical compaction (Figure 29). These fragments have unstable mineral compositions which are compressed easily on undergoing mechanical compaction.

Grain packing can also tell the degree of mechanical compaction, normally closely packed mineral grains are the effect of intense mechanical compaction. And this has been observed on the analysed sandstones of the Aspelintoppen Formation (Figure 31). It shows that compaction has the effect of reorienting grains to attain a close packing fabric. In this type of fabric usually porosity is observed with very low amount.

6.4 Diagenetic Minerals

Authigenic clay

Clay minerals are formed from different chemical reactions that occur in the deposited sediments in near surface condition and some even develop during deep burial by reaction involving detrital and diagenetic minerals with interstitial-water. In most sandstone reservoirs, authigenic clay minerals do occur as pore-filling or replacive of detrital grains.

Kaolinite

The identified kaolinite in sandstones of the Battfjellet Formation occurs as pore filling minerals in most of the analysed sandstone sample. The presence of this mineral in the analysed sandstones indicates the formation experienced near surface reactions in the early diagenesis phase, as it is well known that kaolinite forms during early diagenesis in humid environment and low pH (Worden & Burley, 2003). And it presence in the analysed thin section samples shows that the sandstones of this formation passed warm and humid condition during their early stage of diagenesis.

Normally formation of kaolinite clay mineral involves alteration of detrital mineral fragments with meteoric water, the observed kaolinite in the Battfjellet Formation might have formed from alteration of feldspar and mica when contacted with meteoric water. The Battfjellet Sandstones are being composed with abundant of micaceous metamorphic fragments, biotite and some minor amounts of feldspar which are considered being the possible sources for the formation of the diagenetic mineral kaolinite. Below are chemical reactions responsible for the formation of kaolinite mineral that involve alteration of detrital feldspar and muscovite (Bjørlykke & Jahren, 2010).

$$2K(Na)AlSi_3O_8 + 2H^+ + 9H_2O = Al_2Si_2O_5(OH)_4 + 4H_4SiO_4 + 2K^+(2Na^+)$$

Feldspar Kaolinite silica cations

$$2KAl_3Si_3O_{10}(OH)_2 + 2H^+ + 3H_2O = 3Al_2Si_2O_5(OH)_4 + 2K^+$$

Muscovite Kaolinite

The Batfjellet Sandstones is of shallow marine environment and was deposited in a regression mega sequence. The formation of kaolinite is thought to have been formed during the relative fall of sea level that made meteoric water to reach the marine sediments. The process is known as hydraulic head creation that was responsible for flushing meteoric water to the shallow marine sediments (Mansurbeg, et al., 2013).

The possible impacts of kaolinite in the analysed sandstones are porosity reduction and decrease of permeability. As most of the found kaolinite are pore filling minerals, their presence in the sandstones tends to reduce porosity as they are found occurring in between mineral grains (Figure 17 and Figure 28). The crystals of kaolinite are well recognised to have effect over the quality of the reservoir by plugging pore throats and diminishing reservoir permeability. The effect is most found during production phase as the mineral kaolinite will tend to migrate and plug the pore spaces of the reservoir (Ali, et al., 2010). Furthermore, the precipitation of kaolinite mineral is referred as chemical compaction which have negative effect to the quality of the reservoir.

Illite

As it has been documented in the result that the analysed sandstone of the Battfjellet Formation contains small amounts of illite minerals. Illite is formed in a deep burial where its reaction involves replacement of kaolinite or smectite under high temperatures that is greater than 70°C (Worden & Burley, 2003). Due to the presence of K-feldspar and kaolinite in the analysed sandstone samples of the Battfjellet Formation, illite formation is thought to have originated from reaction of kaolinite and K-feldspar. Below is the reaction showing the formation of illite (Bjørlykke & Jahren, 2010) that is thought to have occurred in the sandstones of Battfjellet Formation.

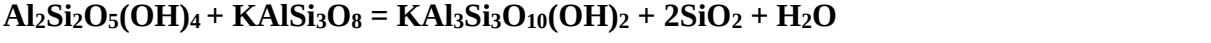

$$Al_2Si_2O_5(OH)_4 + KAlSi_3O_8 = KAl_3Si_3O_{10}(OH)_2 + 2SiO_2 + H_2O$$

Kaolinite K-feldspar illite silica

Illite has characteristics of flakes and filaments like hair crystals in the host reservoir rock which has great effect on the reduction of permeability. It is known as the most permeability reducing factor in the reservoir rock. The same effect can be applied to the Battfjellet Sandstones though the mineral was not found in a large extent, but it proves the sandstones to have reached mesogenesis phase as the formation of this mineral occurs in a deep burial and is controlled by the increase of temperature (Worden & Burley, 2003).

Porosity loss in these sandstones is also contributed by the presence of pore filling illite (Figure 24) as pore sizes are reduced by the presence of this authigenic clay mineral.

Chlorite

The most dominant clay mineral in the analysed sandstone is chlorite, it is found occurring as pore filling and replacive mineral. The origin of this authigenic clay could be from transformation of eogenetic kaolinite clay mineral. As it has been reported that the diagenetic chlorite is formed from replacement of kaolinite in a system having very low potassium as the presence of potassium in system will generate illite on the increase of temperature during deep burial. The process responsible for the formation of chlorite clay mineral from replacing kaolinite mineral occur at temperature of 165-200 °C with depth ranging from 3.5 to 4.5 km (Worden & Burley, 2003). The sandstones of the Battfjellet Formation have found with plentifully amount of kaolinite that are considered as one of the sources of the found chlorite and it can concluded that some of chlorite observed in these sandstones might have been originated from the kaolinite clay mineral.

It has been known that, green marine clay minerals such as berthierine and odinite found in marine facies can develop to chlorite minerals on the increase of temperature during deep burial. These green clay minerals are most found in the deltaic and shallow-marine sandstone (Morad, et al., 2010). Hence the Battfjellet Sandstone is of shallow marine deposits then the concept mentioned here could have been the mechanism for the occurrence of chlorite in the sandstones analysed in this study.

Diagenetic chlorite minerals have the tendency to react with drilling fluids and chemical fluids during treatment of the reservoir. These chemical fluids react with chlorite to produce Fe-hydroxide-gel which can plug and block the pore throats. Therefore, the presence chlorite cement in the sandstone is of great threat when it comes to the quality of the reservoir especially

on part of permeability. Special attention should be carried out on choosing the proper chemical for treatment of the reservoir during the time of drilling and production (Almon & Davies, 1981).

Pore sizes have been reduced due to presence of chlorite, some pores are almost filled by this mineral. Porosity loss has also been contributed from the presence of authigenic chlorite in the pore spaces of the analysed sandstones.

Pyrite

Authigenic pyrite mineral was observed occurring adjacent to diagenetic siderite (Figure 25) though it was found in very small amount. Its formation could have strong relation to the formation of siderite as they both form in anoxic condition with the presence of an aerobic bacteria (Wilkinson, et al., 2000).

Pyrite forms in shallow burial conditions by the reaction involving detrital iron minerals with biogenic H_2S. The presence of organic matter is very important for this reaction to occur as the fact that the organic matter usually act as reducing agents during the reaction with sulphate reducing bacteria to form the H_2S. The process responsible for the formation of pyrite involve iron reducing bacteria, reducing organic matter with the presence of the oxidising sulphate ions and mineral iron cations (Worden & Burley, 2003; Berner, 1984). The pyrite minerals observed in the formation are thought to have formed in the described condition of early diagenetic marine environment.

The content of pyrite in the samples representing the Battfjellet Formation indicates the sediments were deposited in anoxic marine environment in sulphate reduction zone 2 and undergone early near surface chemical reactions in early diagenesis. It also suggests that, sediments were deposited with organic matter together with dissolved sulphate and reactive detrital iron minerals (Berner, 1984; Curtis, 1980).

Siderite

The sandstones of the Battfjellet Formation contain numerous amount of authigenic siderite, it was found as small particles surrounding calcite cements and others were found in large crystals filling the pore spaces (Figure 25 and Figure 26).

The presence of siderite minerals suggests that, the sediments were deposited in marine environment and then cemented in early diagenesis by interaction of sediments with pore fluids. The siderite was found exhibited the same style as the one observed by Mansurbeg, et al., (2013) in Eocene Sandstones of the Tertiary Central Basin. The mineral was found as disseminated grains coating detrital carbonate.

The authigenic siderite has been formed by the presence of Iron reducing bacteria and organic matter in anoxic marine condition by the process known as microbial Fe(III) reduction (Ellwood, et al., 1988; Roh, et al., 2003). The process involved a crystalline and amorphous Fe(III)-oxide reduced to Fe(II)-ion and Fe minerals under anaerobic conditions. The reaction requires the presence of CO_2 to form aqueous bicarbonate concentration that is important in the formation of siderite precipitates.

The formation of siderite occurs only when the rate of Fe production exceeds the rate of sulphide production. So, when Fe reduction is so week the system will favour formation of pyrite (Wilkinson, et al., 2000). Likewise, Worden & Burley, 2003 suggested the that eogenetic siderite develops in a system rich with reduced iron with very low amounts of marine constituents. They also mentioned the authigenic siderite normally form at sequence boundary and in flooding surface at a time of low sedimentation rate.

Therefore, the Battfjellet Formation is assumed being developed in a reduced system having high production rate of Fe that facilitated the formation of siderite mineral.

Calcite

Carbonate cement found was identified as calcite and was observed in the pore spaces of the sandstone. The cement was observed in sample LY95-2 and LY95-6L as shown in Figure 28.

The calcite cementation was observed in both formations of the Battfjellet and Aspelintoppen Formation. The presence of this mineral indicates sediments were deposited with carbonate grains that acted as nuclei and facilitated the growth of calcite cement (Morad, et al., 2010).

Calcite cementation found in sandstone of the Battfjellet Formation suggests that sediments were deposited in marine environment and the source of detrital carbonate grains were from wave reworking of shelf carbonate (Mansurbeg, et al., 2013). The texture identified which is microcrystalline implies the cement was formed in early diagenesis.

Chalcedony

The occurrence of biogenic chalcedony cement in the sampleof the Battfjellet Formation indicates the source of cements were from siliceous bioclasts. Precipitation of chalcedonic quartz cement is thought to occur in early diagenesis as dissolution of these chemically unstable grains and precipitation of cements occurred in early deposition time of sediments (Morad, et al., 2010).

Quartz

The observed quartz cement in the sandstones of the Battfjellet and Aspelintoppen Formation indicates that the sandstones were buried deep enough to form quartz cement, as quartz precipitation occurs at temperature greater than 70 °C. The presence of this cement proves that, it was formed in mesogenesis regime (Worden & Burley, 2003). The cement was identified in small proportions and it was hard to differentiate it from detrital quartz grains.

A possible source for the quartz cement in the analysed sandstones is from the reaction responsible for formation of illite, where kaolinite and potassium feldspar reacted to form illite and silica, and then silica precipitate over the detrital quartz to form quartz cement.

6.5 Paragenetic Sequence

A Paragenetic sequence of the minerals formed in the Battfjellet sediments from Nordenskiöldfjellet area is thought to start with mechanical compaction, then followed with precipitation of authigenic pyrite, siderite, kaolinite, calcite, chalcedony, quartz, illite and ended with chlorite. The paragenetic sequence have been obtained based on petrographic studies conducted in this study and theories of origin of diagenetic minerals conducted before

in various studies. The sequence presented below (Figure 30) has been suggested by Mansurbeg, et al., (2013) on the study conducted in the Eocene sandstone of Tertiary Central Basin, Spitsbergen which match to the minerals identified in the sandstones of the Battfjellet and Aspelintoppen Formation.

The observed diagenetic minerals in the sandstone of Aspelintoppen Formation are siderite and calcite that are interpreted to have been formed in early diagenesis whereas quartz cement found has been formed in deep burial.

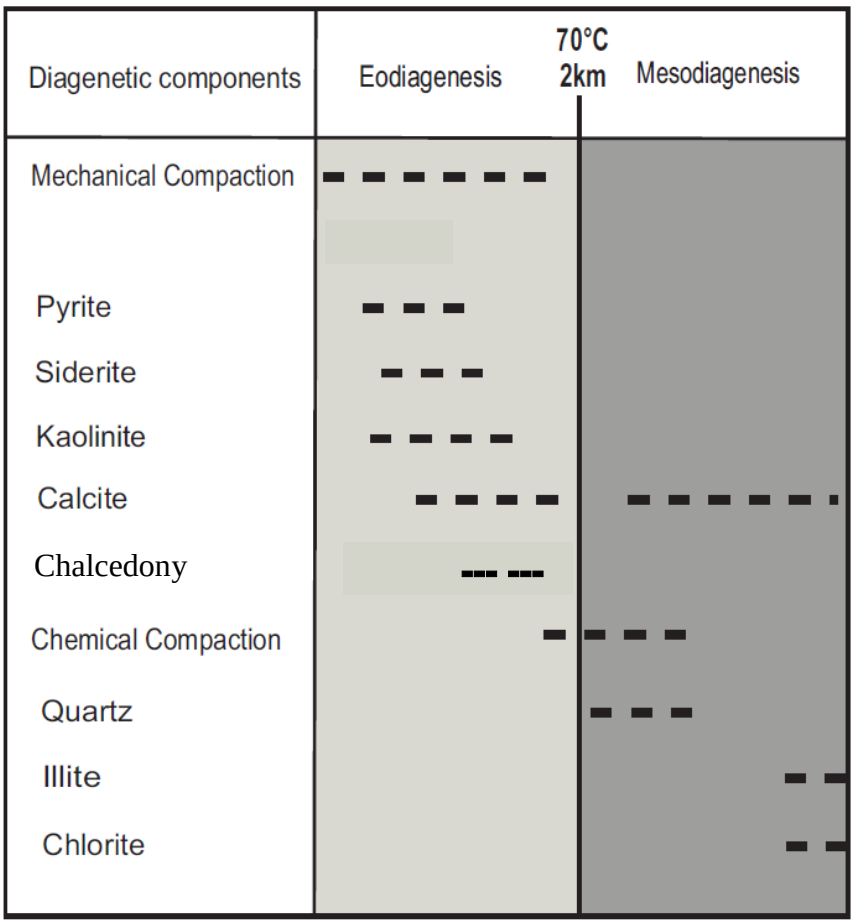

Figure 30: A modified paragenetic sequence of mineral formed in the sandstones of the Battfjellet Formation (Mansurbeg, et al., 2013).

6.6 Reservoir Properties

The Battfjellet Formation has been found with an intermediate total porosity ranging from 8.72 to 13.57%. Porosity analysis was conducted on different parts of thin section samples, the grey areas that present porosity in optical micrography images include some part of minerals that make porosity estimation being a little higher as compared to the values obtained from SEM BEI analysis. The observed porosity is of intergranular type that is found occurring in between mineral grains. The area fraction measurement was conducted with imagej software and measured porosity seem to be reasonable as compared with the one analysed with an eye optical observation on the thin section samples.

The coarse grain sandstones of sample LY95-3 and LY95-5 display slightly higher porosity as compared to the fine-grained sandstones of sample LY95-7, LY95-6-T, LY95-6-L, and those of Aspelintoppen Formation (LY95-2 and LY95-1).

As it has been presented before that the Battfjellet Formation is of shallow marine origin deposited in regression sequence, its sedimentological configuration has played a big role to the porosity available in the Eocene Sandstones. Such sedimentological characteristics are degree of sorting, grain shape, roundness and grain packing.

Sorting of the grains have been observed and found to be poor as there are mixing of grains and some rock fragments of different sizes in the sandstones analysed. Some samples were found having a moderate sorting with some amount of porosity. Porosity is strongly related with degree of sorting as well-sorted sandstone usually has good porosity. Poor sorted sandstones are characterised with low porosity, as what is observed in this fine sandstone of sample LY95-7, LY95-6-T and LY95-6L.

Coarse-grained sandstone of sample LY95-5 and LY95-3 are characterised with angular to subangular mineral grains that might have contributed to the moderate porosity found. The roundness of the composed grains add value to the porosity by increasing porosity and permeability. Porosity will always be expected high in the rock composed with angular grains as they create pore bridging that lead to the sandstones attaining a looser packing (Beard & Weyl, 1973). The theory mentioned here can be related and explain amount of the porosity found in the coarse-grained sandstone of the Battfjellet Formation.

Porosity loss in the sandstone samples have been contributed by the presence of ductile grains such as micaceous fragments, mica and detrital chlorite. Mechanical compaction cause volume reduction of compacted rock/ sediments as the forces responsible squeeze together sediments and mineral grains to attain more closely packed arrangement. As it has been reported before that ductile mineral grains will tend to be affected more during compaction, it is well known that these grains are soft and delicate which make them more vulnerable to the compaction (Mansurbeg, et al., 2013).

Mansurbeg, et al., (2013) described that one of the reasons porosity was found low in Eocene Sandstones of the Tertiary Central Basin, Spitsbergen was the presence of ductile mineral grains. Mechanical compaction destroyed primary porosity of the Eocene Sandstones as ductile rock fragments were more compressible during the compaction. The Battfjellet and Aspelintoppen sandstone in the Nordenskiöldfjellet have the same ductile minerals grains as the ones found in the Eocene sandstone described by Mansurbeg, et al., (2013) found in the Van Keulen Fjord area.

The sandstone of the Battfjellet and Aspelintoppen formation show low porosity and are dominated with these ductile mineral grains. Therefore, mechanical compaction can be considered as one of the reason porosity is low in the analysed sandstones in the Aspelintoppen and in some sandstones of the Battfjellet Fromation.

Chemical compaction can also be considered as the reason of reduction of the porosity in sandstones analysed in both formations. Cementation has the tendency of reducing porosity volume as authigenic mineral precipitate around mineral grains and can sometime fill the entire pores of sedimentary rock.

Sample LY95-7, LY95-6-T and LY5-6-L from the Battfjellet Formation were observed with diagenetic alteration of illite, kaolinite, chlorite, calcite and siderite. The presence of these cements contributed to the reduction of porosity. The sandstones are most dominated with authigenic kaolinite and chlorite occurring as pore filling mineral that tend to reduce the primary porosity. The other diagenetic cements were found in very minor trace amount and contribute low in porosity loss.

Samples LY95-3 and LY95-2 from the Aspelintoppen Formation are very fine-grained and showing very low porosity. Again, the poor porosity observed was contributed by mechanical compaction that affected ductile mineral fragment.

Chemical compaction (cementation) has contributed in low amount on reduction of porosity as minor trace amount of carbonate cement have been identified in the sandstone from these two formations. The observed cements were found in low amounts patchily distributed in the pore spaces of the sandstones.

7. CONCLUSION

The shallow marine sandstones of the Battfjellet Formation have found being mineralogy and textural immature with diagenetic alteration of pyrite, siderite, kaolinite, calcite, chalcedony, quartz, illite and chlorite. The sandstones have passed eogenetic and mesogenetic zones and this is evidence with early formation of pyrite, siderite and calcite cement where burial diagenesis is evidenced with the formation of quartz, illite and chlorite.

Porosity loss has been contributed by mechanical compaction that affected lithic rock fragments available in the Battfjellet Sandstones, the compaction was evidenced with the deformation of minerals grains. Chemical compaction has also contributed to the reduction of porosity, as most of the pore spaces were found filled with kaolinite and chlorite clay minerals.

The Aspelintoppen Sandstones are of terrestrial deposits deposited in a deltaic plain system. The sandstones in this formation are chemically and textural immature found with diagenetic alteration of siderite, calcite and quartz. Porosity loss was caused by mechanical compaction that affected lithic rock fragments found in these sandstones as they were found deformed and fractured. Chemical compaction has noticed to have played important role on the destruction of porosity and led to the porosity observed being low. The sandstones are characterized with the diagenetic minerals formed during eogenetic and mesogenetic zone.

Sandstones from both formations are believed to have originated from metamorphic, igneous and sedimentary provenance of west Spitsbergen thrust fold.

8. REFERENCES

Ali, S. A., Clark, W. J., Moore, W. R. & Dribus, J. R., 2010. Diagenesis and reservoir quality. *Oilfield Review,* Volume 22, pp. 14--27.

Allen, . P. A. & Allen, J. R., 2013. *Basin analysis: Principles and application to petroleum play assessment.* s.l.:John Wiley \& Sons.

Almon, W. & Davies, D., 1981. Formation damage and the crystal chemistry of clays, ch.5,. *Clays and Resource geologists.,* pp. p. 81-103.

Apted, M. J. & Liou, J., 1983. Phase relations among greenschist, epidote-amphibolite, and amphibolite in a basaltic system. *American Journal of Science,* Volume 283, pp. 328--354.

Beard, D. & Weyl, P., 1973. Influence of texture on porosity and permeability of unconsolidated sand. *AAPG bulletin,* Volume 57, pp. 349--369.

Berner, R. A., 1984. Sedimentary pyrite formation: an update. *Geochimica et cosmochimica Acta,* Volume 48, pp. 605--615.

Bjørlykke, K., Nedkvitne, T., Ramm , M. & Saigal, 1992. Diagenetic processes in the Brent Group (Middle Jurassic) reservoirs of the North Sea: an overview. *Special Publications,* pp. 61, 263-287..

Bjørlykke, K. & Jahren, J., 2010. Sandstones and Sandstone Reservoirs, Chapter 4 in K. Bjørlykke (ed.). *Petroleum Geoscience: From Sedimentary Environments to Rock Physics,* pp. 113-140.

Curtis, C., 1980. Diagenetic alteration in black shales. *Journal of the Geological Society,* Volume 137, pp. 189--194.

Dallmann, W. K., 1999. Lithostratigraphic lexicon of Svalbard: review and recommendations for nomenclature use: Upper Palaeozoic to Quaternary bedrock.

Dutton, S. P., White, C. D., Willis , B. J. & Novakovic, D., 2002. Calcite cement distribution and its effect on fluid flow in a deltaic sandstone, Frontier Formation, Wyoming. *AAPG bulletin,* pp. 2007--2021.

Ellwood, B. B. et al., 1988. Siderite formation in anoxic deep-sea sediments: A synergetic bacteria controlled process with improtant implications in paleomagnetism. *Geology,* Volume 16, pp. 980--982.

Folk, R. L., 1951. Stages of textural maturity in sedimentary rocks. *Journal of Sedimentary Research,* Volume 21.

Galiatano, H. I., 2017. *A reconnaissance study on Diagenesis and Reservoir properties of sandstones of the Battfjellet and Aspelintoppen Formation from Nordenskiöldfjellet, Svalbard.,* Trondheim: s.n.

Gobbett, D. J., 1963. Carboniferous and Permian brachiopods of Svalbard.

Helland-Hansen, W., 1990. Sedimentation in Paleogene Foreland Basin, Spitsbergen (1). *AAPG Bulletin,* Volume 74, pp. 260--272.

Helland-Hansen, W., 2010. Facies and stacking patterns of shelf-deltas within the Palaeogene Battfjellet Formation, Nordenski{\"o}ld Land, Svalbard: implications for subsurface reservoir prediction. *Sedimentology,* Volume 57, pp. 190--208.

Kellogg, H. E., 1975. Tertiary stratigraphy and tectonism in Svalbard and continental drift. *AAPG Bulletin,* Volume 59, pp. 465--485.

Klein, C., 1993. *Manual of mineralogy.* s.l.:s.n.

Kozak, K. et al., 2013. Analytical studies on the environmental state of the Svalbard Archipelago provide a critical source of information about anthropogenic global impact. *TrAC Trends in Analytical Chemistry,* Volume 50, pp. 107--126.

Mansurbeg, H. et al., 2013. Diagenetic alterations related to falling stage and lowstand systems tracts of shelf, slope and basin floor sandstones (Eocene Central Basin, Spitsbergen). *Linking Diagenesis to Sequence Stratigraphy,* pp. 353--378.

McBride, E. F., 1963. A classification of common sandstones. *Journal of Sedimentary Research.*

Morad, S., Al-Ramadan, K., Ketzer, J. M. & De Ros, L., 2010. The impact of diagenesis on the heterogeneity of sandstone reservoirs: A review of the role of depositional facies and sequence stratigraphy. *AAPG bulletin,* Volume 94, pp. 1267--1309.

Muller, . D. R. & Spielhagen, R. F., 1990. Evolution of the Central Tertiary Basin of Spitsbergen: towards a synthesis of sediment and plate tectonic history. *Palaeogeography, Palaeoclimatology, Palaeoecology,* Volume 80, pp. 153-172.

Roh, Y. et al., 2003. Biogeochemical and environmental factors in Fe biomineralization: magnetite and siderite formation. *Clays and Clay Minerals,* pp. 83--95.

Steel, R. et al., 1985. The Tertiary strike-slip basins and orogenic belt of Spitsbergen.

Steel, R., 1977. Observations on some Cretaceous and Tertiary sandstone bodies in Nordenskiold Land, Svalbard}. *Nor. Polarinst. {\AA}rbok 1976,* pp. 43--67.

Steel, R., Dalland, A., Kalgraff , K. & Larsen, V., 1981. The Central Tertiary Basin of Spitsbergen: sedimentary development of a sheared-margin basin.

Steel, R., Dalland, A., Kalgraff, K. & Larse, 1981. The Central Tertiary Basin of Spitsbergen: sedimentary development of a sheared-margin basin.

Talwani, M. & Eldholm, O., 1997. Evolution of the Norwegian-Greenland sea. *Geological Society of America Bulletin,* Volume 88, pp. 969--999.

Uroza, C. A. & Steel, R. J., 2008. A highstand shelf-margin delta system from the Eocene of West Spitsbergen, Norway. *Sedimentary Geology,* Volume 203, pp. 229--245.

Volkmar, S. & David, A. M., 1979. The role of secondary porosity in the course of sandstone diagenesis.

Wilde, S. A., Valley, J. W., Peck , W. H. & Graham, C. M., 2001. Evidence from detrital zircons for the existence of continental crust and oceans on the Earth 4.4 Gyr ago. *Nature*, Volume 409, p. 175.

Wilkinson, M., Haszeldine, R., Fallick, A. & Osborne, M., 2000. Siderite zonation within the Brent Group: microbial influence or aquifer flow?. *Clay Minerals*, Volume 35, pp. 107--118.

Worden, R. & Burley, S., 2003. Sandstone diagenesis: the evolution of sand to stone. *Sandstone Diagenesis: Recent and Ancient*, Volume 4, pp. 3--44.

Worsley, D., 2008. The post-Caledonian development of Svalbard and the western Barents Sea. *Polar Research*, Volume 27, pp. 298--317.

Worsley, D., 2008. The post-Caledonian development of Svalbard and the western Barents Sea. *Polar Research*, Volume 27, pp. 298--317.

Ytreland, G., 1980. *Sedimentation along the western margin of the Central Tertiary basin,(Firkanten Formation), Spitsbergen*, s.l.: Thesis. Geol. Inst. Univ. Bergen.

9. APPENDIX

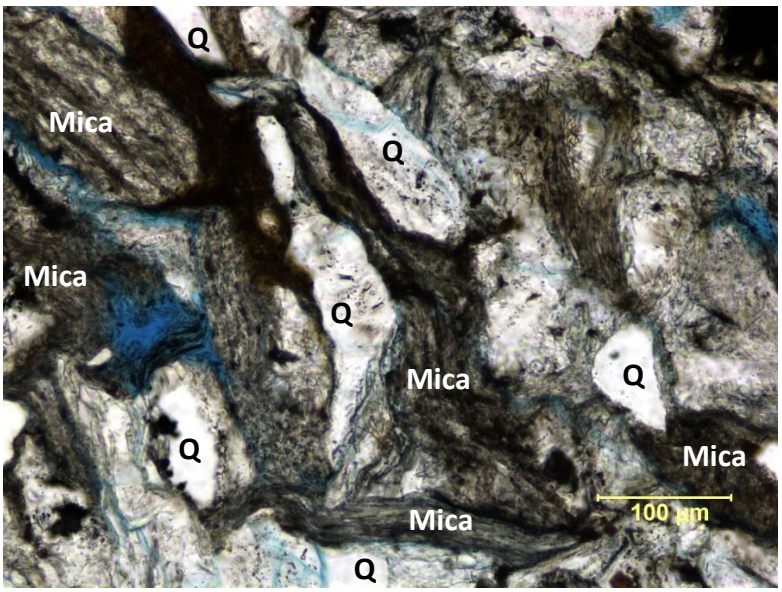

Figure 31:A densely packed mineral grains of quartz and mica fragments in a sample LY95-2.

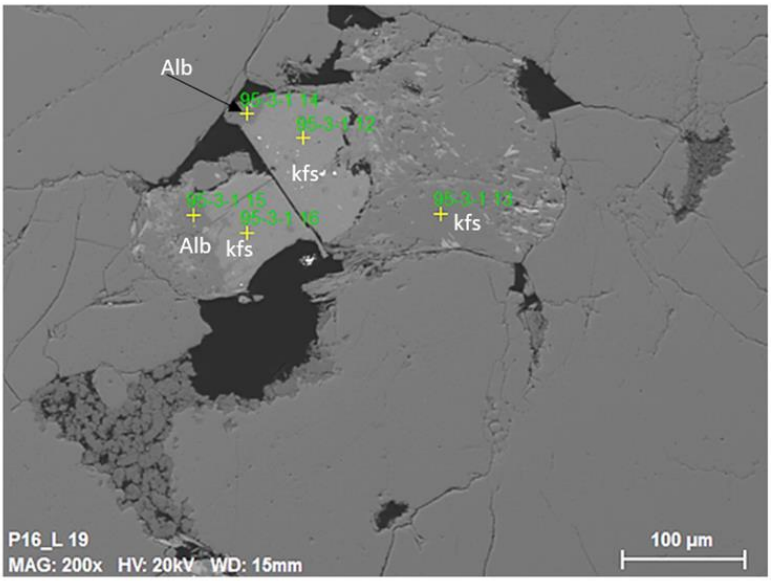

Figure 32: Backscattered Electron image with mineral assemblage of k-feldspar (kfs), albite (Alb), in a thin section sample number LY95-3.

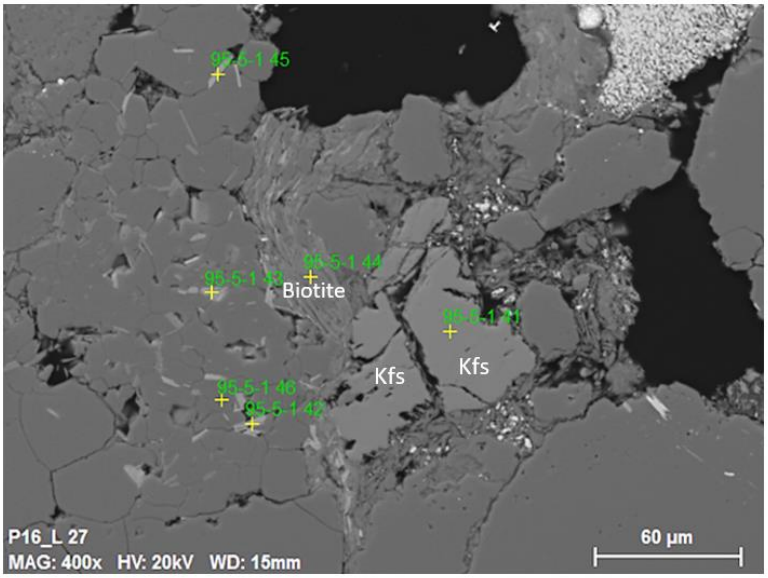

Figure 33: A BEI with some chlorite mineral replacing detrital quartz minerals in a sample LY95-5.

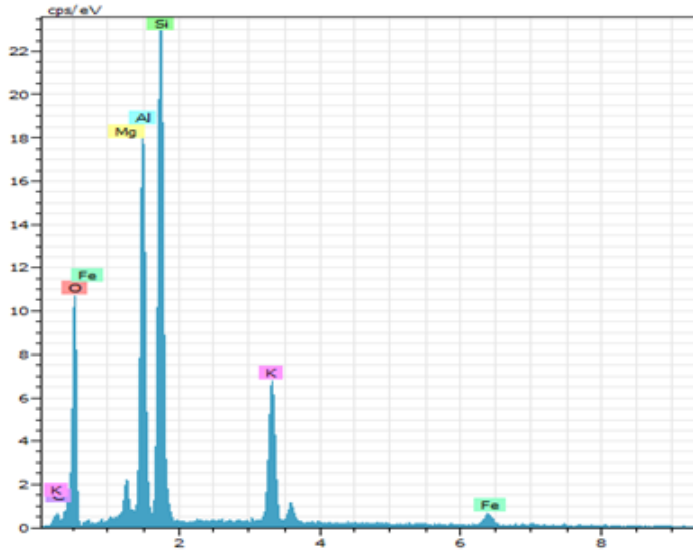

*Figure 34: Biotite (***K(Mg,Fe)$_3$(AlSi$_3$O$_{10}$)(F,OH)$_2$***) mineral examined in EDS.*

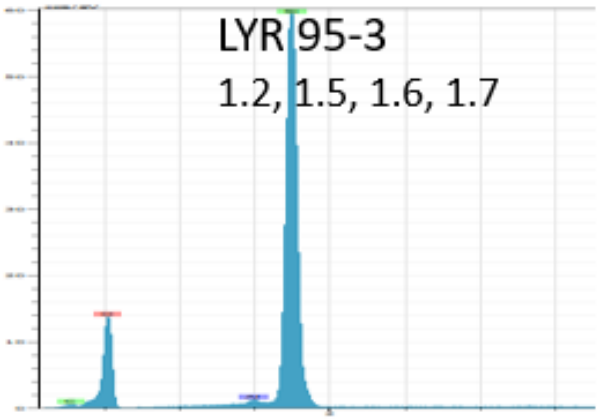

*Figure 35: Energy dispersive spectral showing chemical elemental composition of quartz mineral (**SiO_2**).*

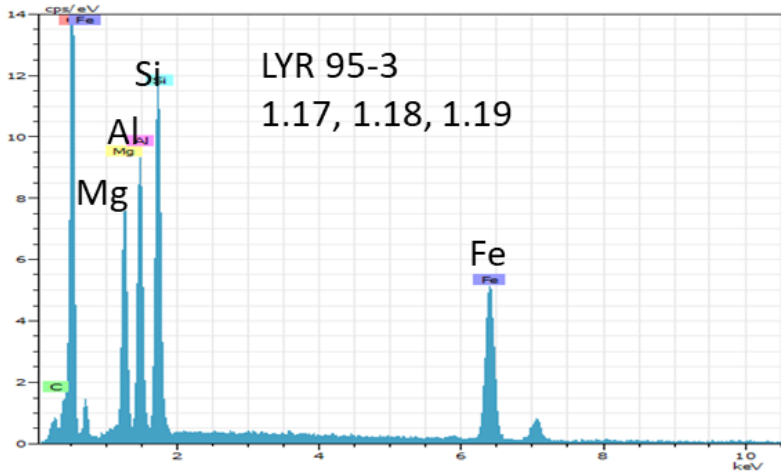

*Figure 36: Energy dispersive spectral (EDS) with chemical elemental composition of chlorite mineral [**(Mg,Fe)3(Si,Al)4O10**].*

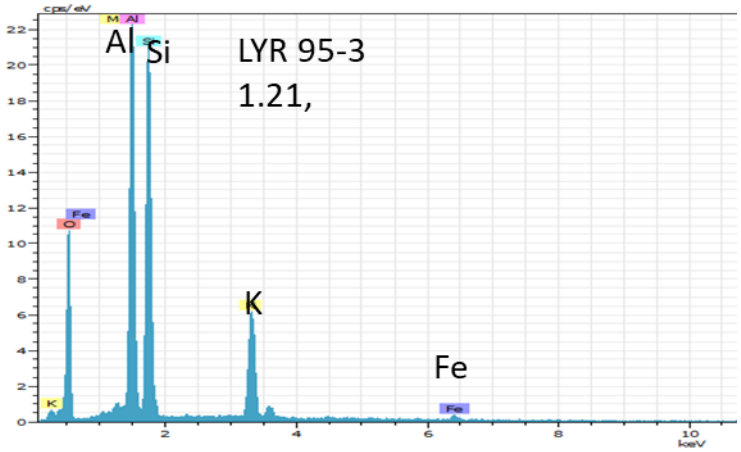

*Figure 37: Energy dispersive spectral (EDS) with chemical elemental composition of muscovite mineral (**$KAl_3Si_3O_{10}(OH)_2$**).*

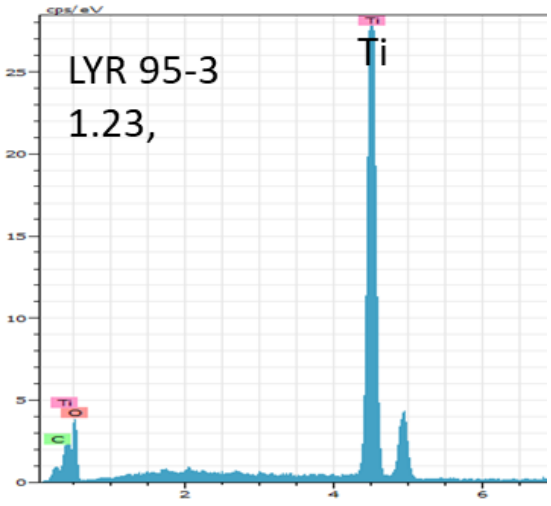

*Figure 38: Energy dispersive spectral (EDS) with chemical elemental composition of rutile **(TiO_2).***

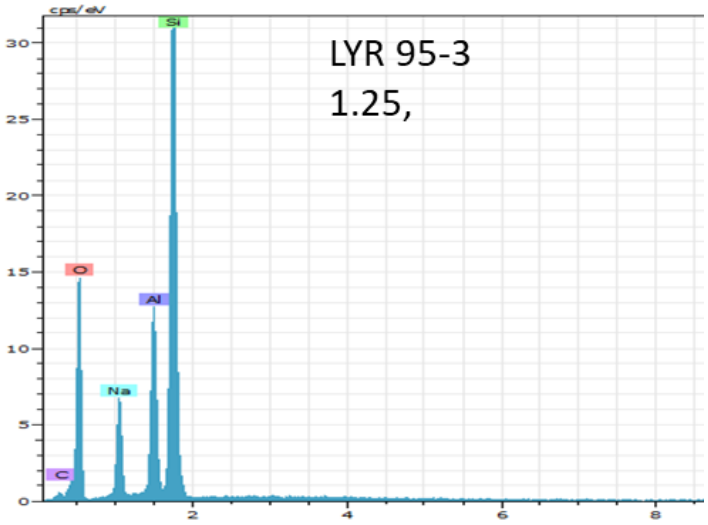

*Figure 39: Energy dispersive spectral (EDS) with chemical elemental composition of albite mineral (**$NaAlSi_3O_8$**).*

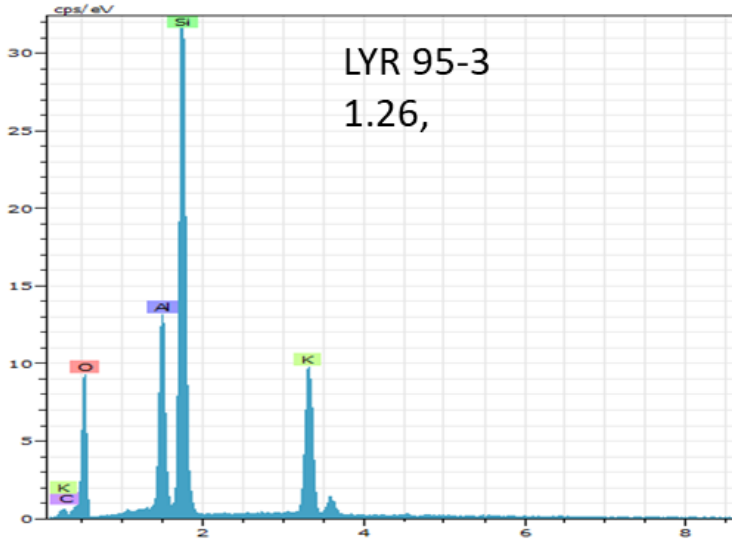

*Figure 40: Energy dispersive spectral (EDS) with chemical elemental composition of k-feldspar mineral (**$KAlSi_3O_8$**).*

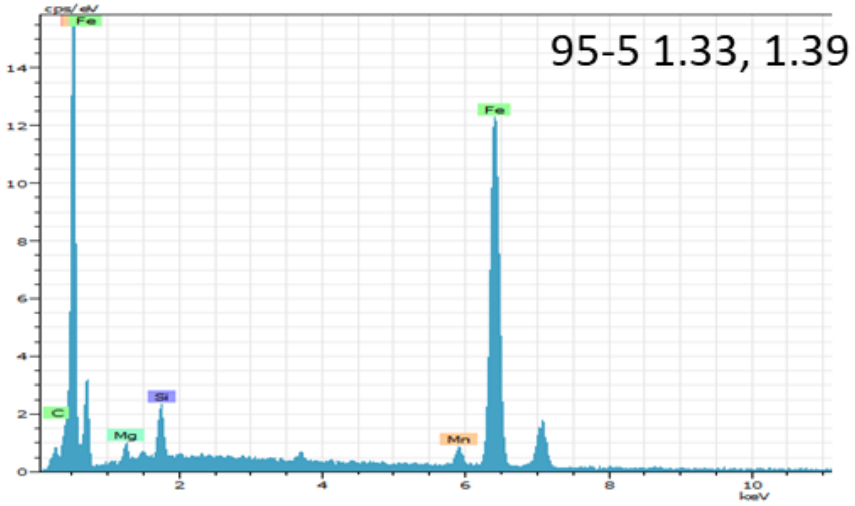

*Figure 41: Energy dispersive spectral (EDS) with chemical elemental composition of siderite (**$FeCO_3$**) occurring with other elements.*

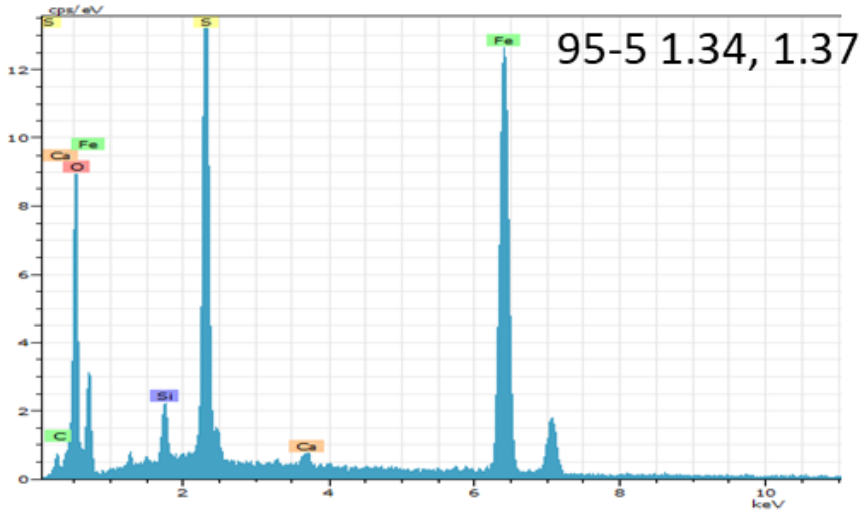

*Figure 42: Energy dispersive spectral (EDS) with chemical elemental composition of pyrite (**FeS**) and mixed carbonate.*

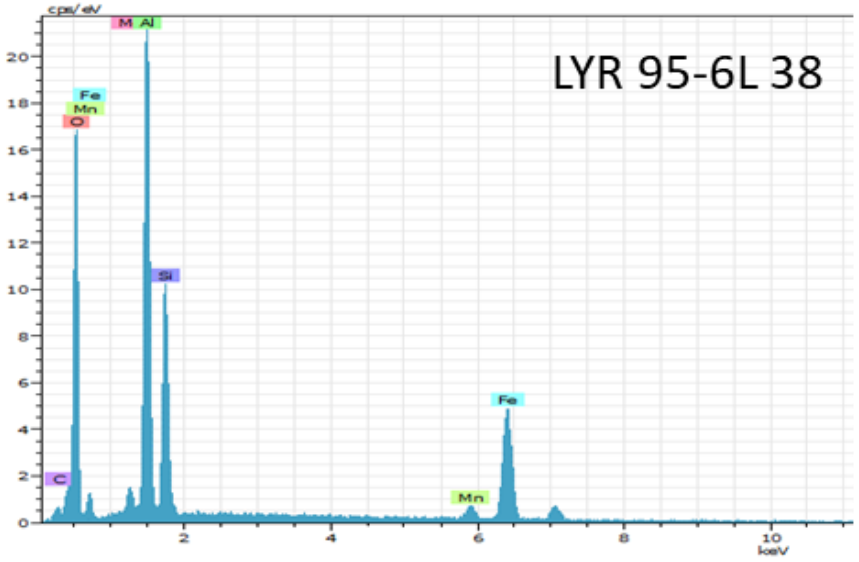

*Figure 43 Energy dispersive spectral (EDS) with chemical elemental composition of epidote mineral [**$Ca_2(Fe,Al)Al_2(SiO_4)(Si_2O_7)O(OH)$**].*

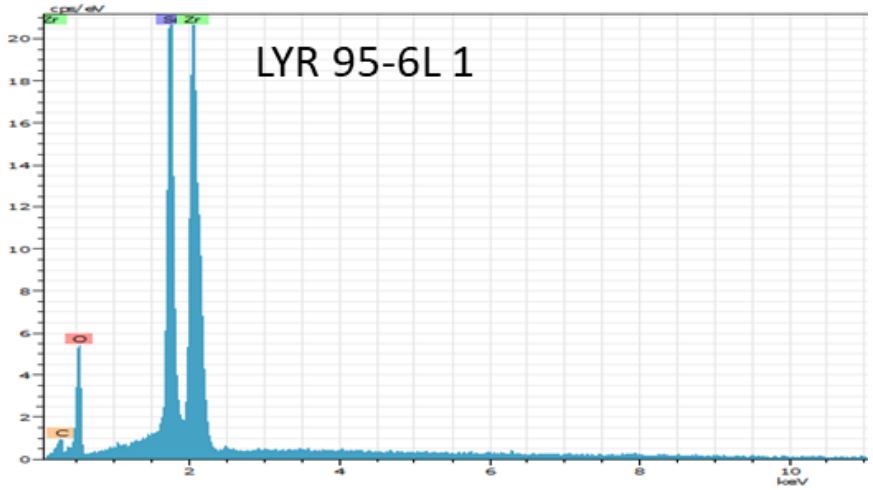

*Figure 44: Energy dispersive spectral (EDS) with chemical elemental composition of zircon mineral **($ZrSiO_4$)**.*

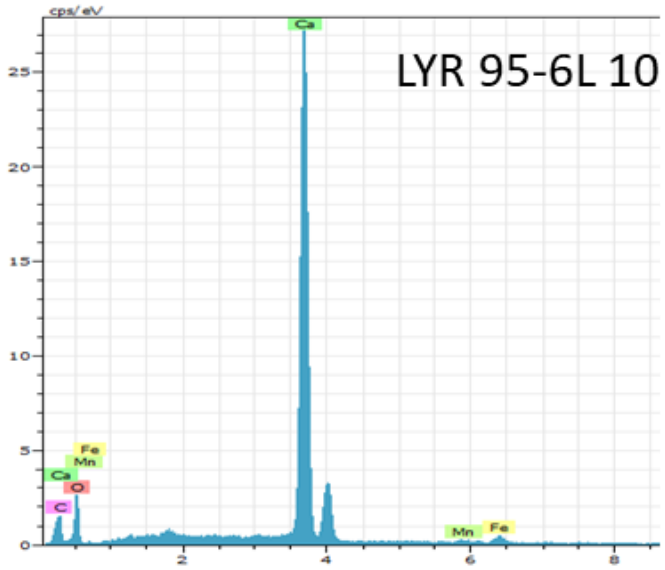

Figure 45: Energy dispersive spectral (EDS) with chemical elemental composition of calcite mineral ***($CaCO_3$)***.

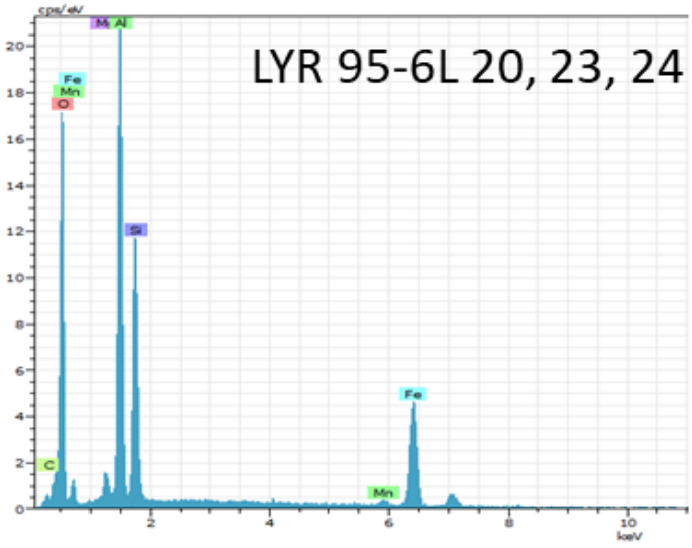

*Figure 46: Energy dispersive spectral (EDS) with chemical elemental composition of chlorite mineral [****(Mg,Fe)3(Si,Al)4O10****].*

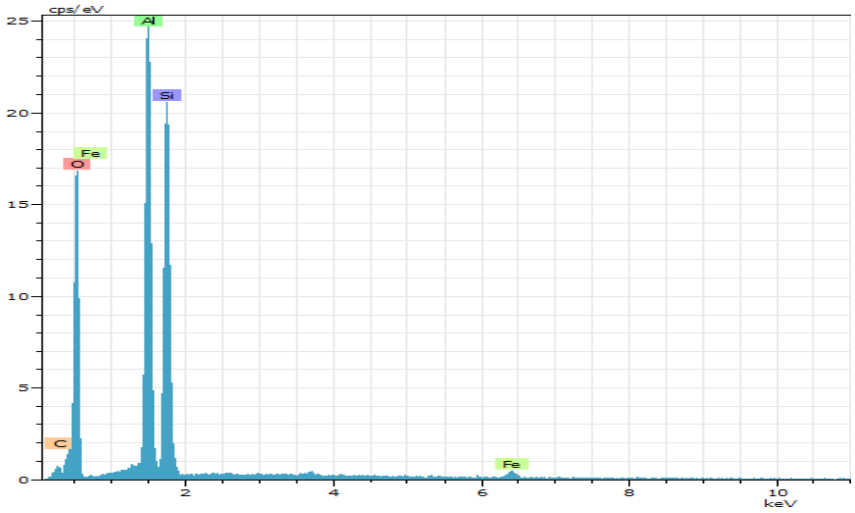

*Figure 47: Kaolinite clay mineral displayed in energy dispersive spectral (**$Al_2Si_2O_5(OH)_4$**).*

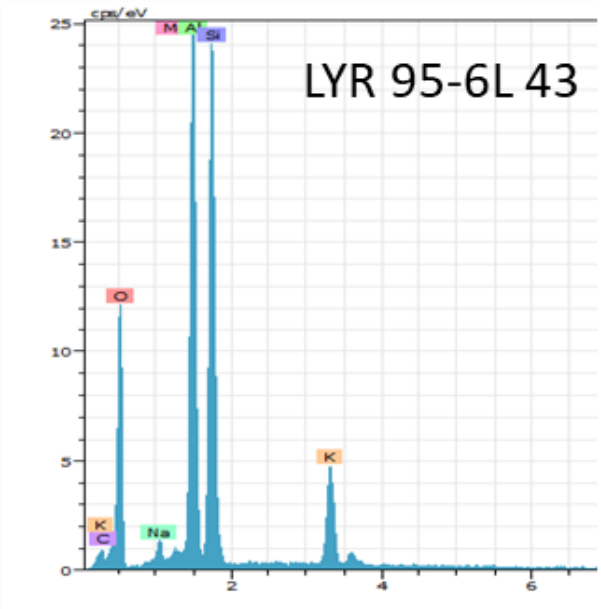

*Figure 48: Energy dispersive spectral (EDS) with chemical elemental composition of illite clay mineral **$(K(Na,Ca)Al_{1.3}Fe_{0.4}Mn_{0.2}Si_{3.4}Al_{0.6}O_{10}(OH)_2)$**.*

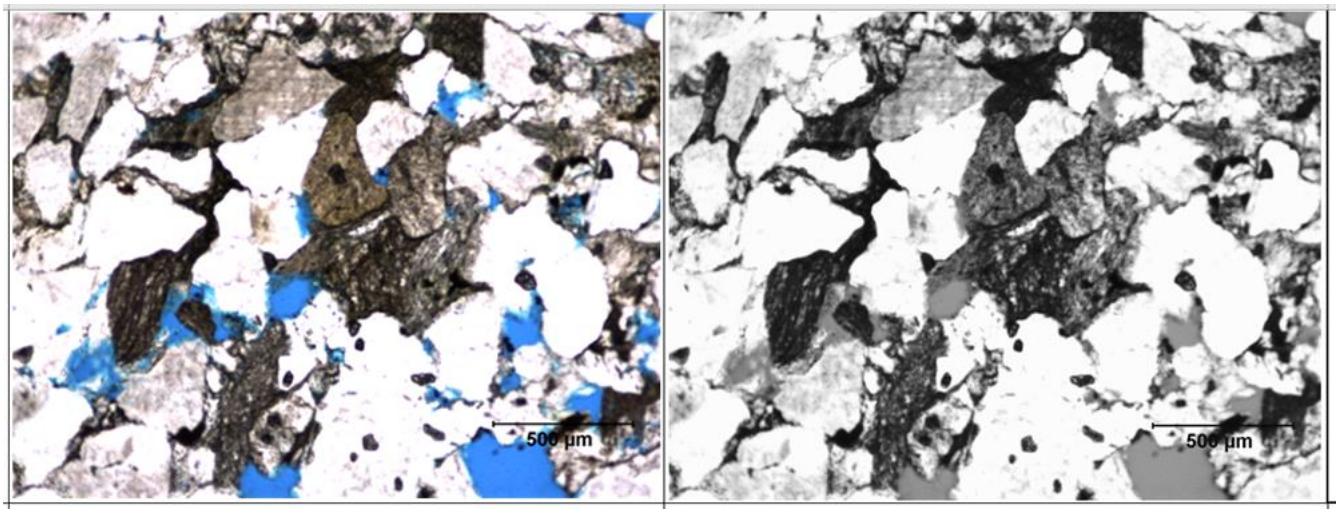

Figure 49: A polished thin section sample number LY95-3 under plane polarized light with its correspondingly black and white image showing porosity in grey colour.

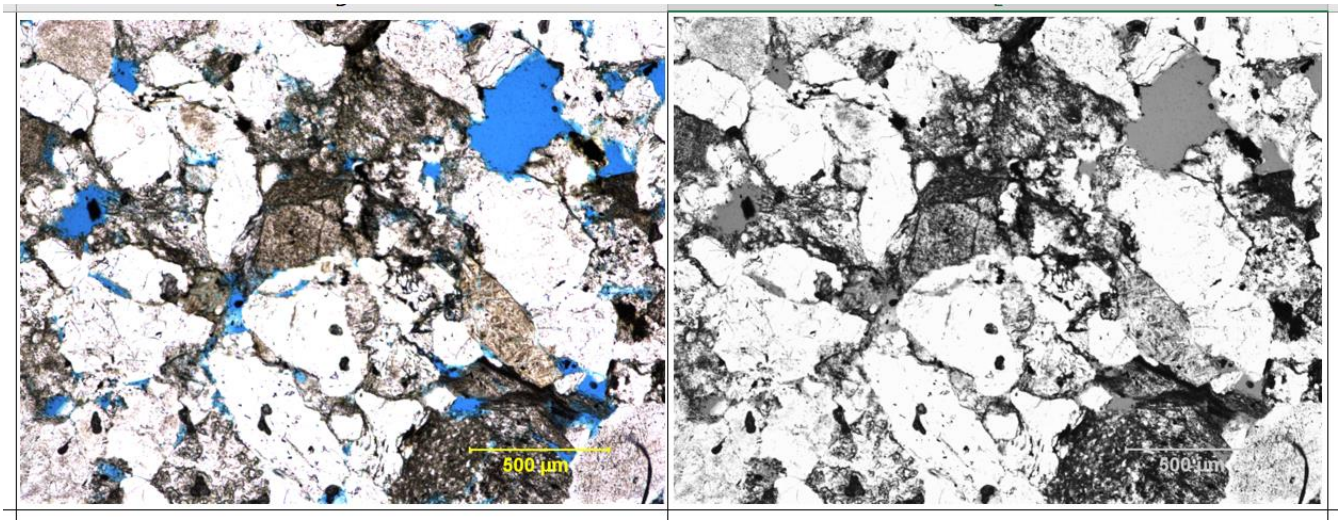

Figure 50: A polished thin section sample number LY95-3 under plane polarized light with its correspondingly black and white image showing porosity in grey colour.

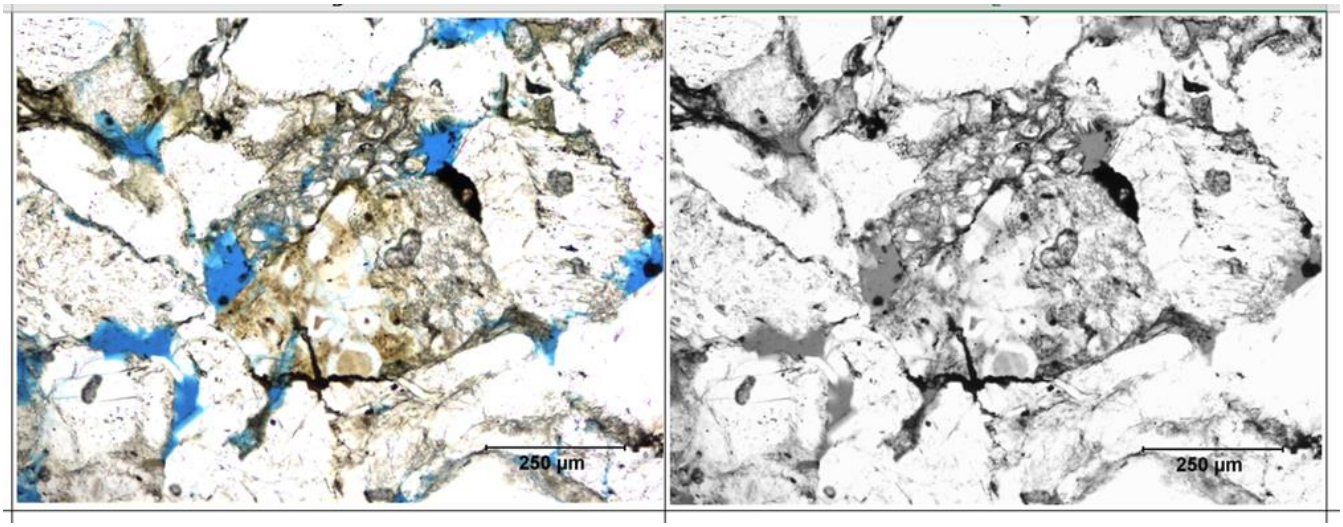

Figure 51:A polished thin section sample number LY95-3 under plane polarized light with its correspondingly black and white image showing porosity in grey colour

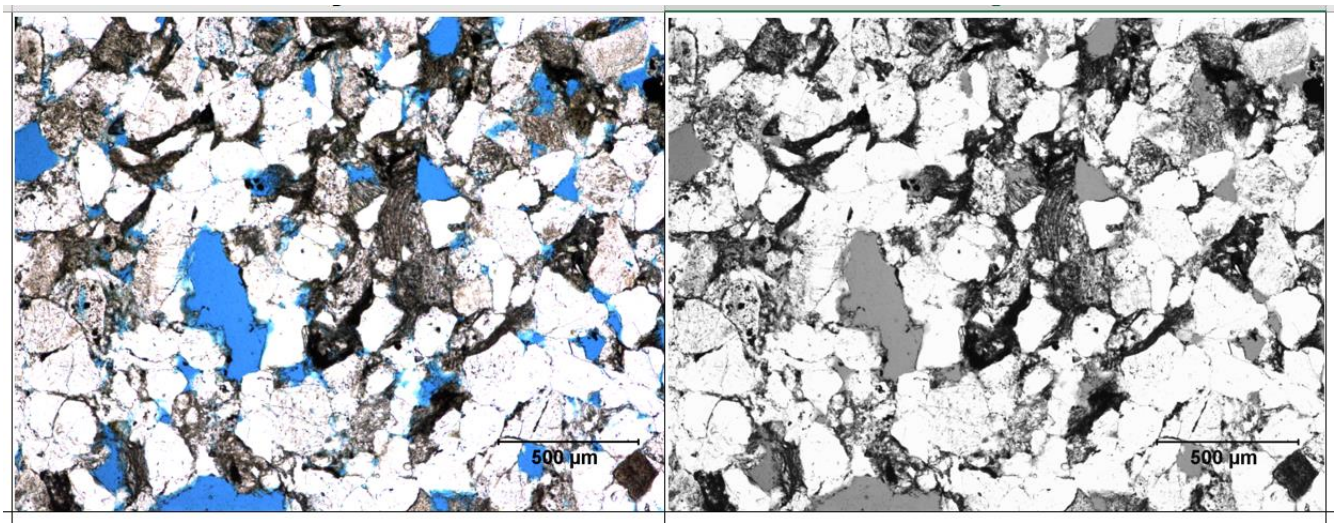

Figure 52: A polished thin section sample number LY95-5 under plane polarized light with its correspondingly black and white image showing porosity in grey colour.

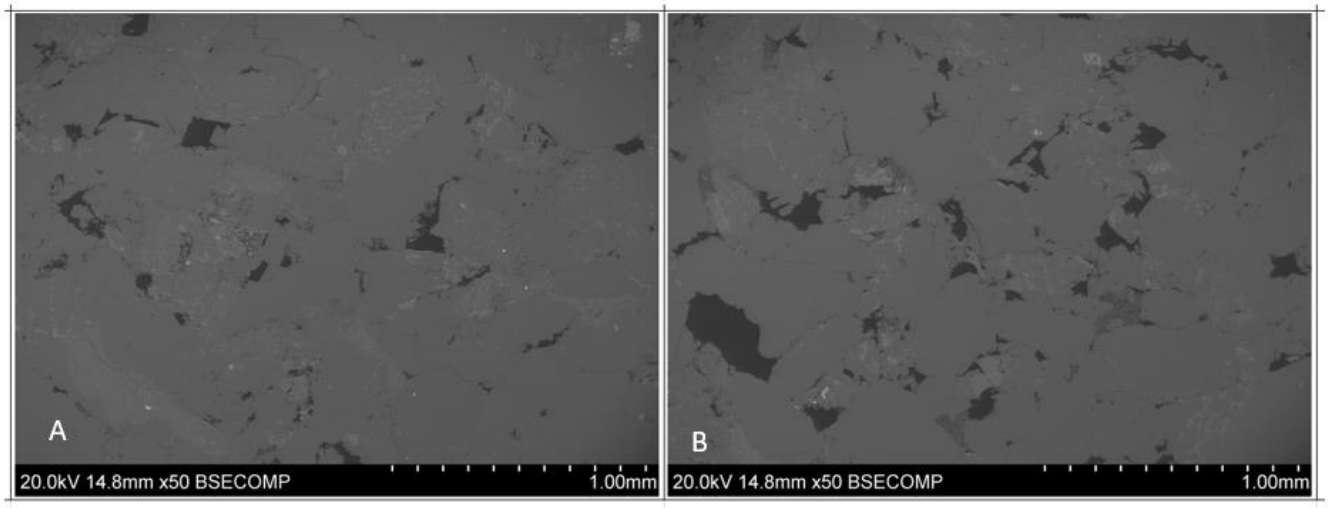

Figure 53: The SEM images (A&B) used for calculation of porosity by using Imagej software, The Image A shows 8.32% porosity and the other image displays 10.93% porosity.

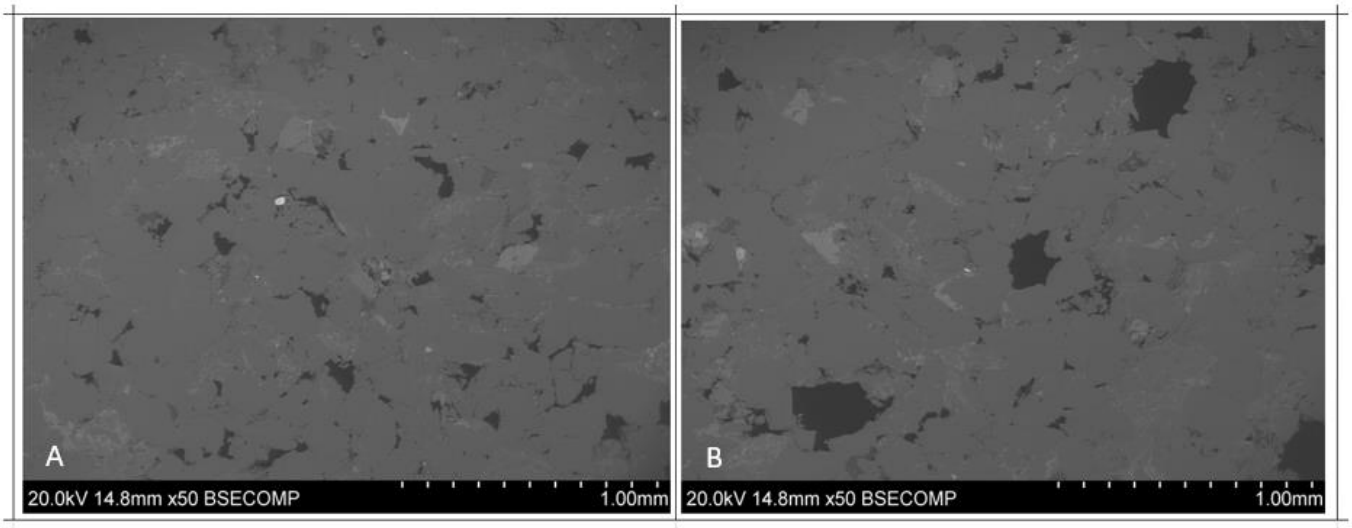

Figure 54: The SEM images (A&B) that have been used for calculation of porosity by using Imagej software, The Image A shows 8.72% porosity and the other image B dispalys 11.09% porosity.

NTNU